




Simbakubwa kutokaafrika, gen. et sp. nov. (Hyainailourinae, Hyaenodonta, 'Creodonta,' Mammalia), a gigantic carnivore from the earliest Miocene of Kenya

Matthew R. Borths & Nancy J. Stevens

To cite this article: Matthew R. Borths & Nancy J. Stevens (2019): *Simbakubwa kutokaafrika*, gen. et sp. nov. (Hyainailourinae, Hyaenodonta, 'Creodonta,' Mammalia), a gigantic carnivore from the earliest Miocene of Kenya, Journal of Vertebrate Paleontology, DOI: [10.1080/02724634.2019.1570222](https://doi.org/10.1080/02724634.2019.1570222)

To link to this article: <https://doi.org/10.1080/02724634.2019.1570222>




View supplementary material 



Published online: 17 Apr 2019.



Submit your article to this journal 



Article views: 195



View Crossmark data 

SIMBAKUBWA KUTOKAAFRICA, GEN. ET SP. NOV. (HYAINAILOURINAE, HYAENODONTA, 'CREODONTA,' MAMMALIA), A GIGANTIC CARNIVORE FROM THE EARLIEST MIOCENE OF KENYA

MATTHEW R. BORTHS * and NANCY J. STEVENS 

Department of Biomedical Sciences, Heritage College of Osteopathic Medicine, Ohio Center for Ecology and Evolutionary Studies, Ohio University, Athens, Ohio 45701, U.S.A., matthew.borths@duke.edu; stevensn@ohio.edu

ABSTRACT—Hyainailourine hyaenodonts are among the largest terrestrial carnivorous mammals known. The clade is widely dispersed, found in Eurasia, North America, and Afro-Arabia in the Paleogene and early Neogene. In this study, we describe dental and postcranial material from *Simbakubwa kutokaafrika*, gen. et sp. nov., the most complete hyainailourine known from sub-Saharan Africa. The material is from a relatively young adult from the early Miocene locality of Meswa Bridge, Kenya. *Simbakubwa* differs from *Hyainailouros* in exhibiting lingually oriented molar protocones, gracile metastyles, and buccolingually compressed, shearing canines. Like other large Miocene hyainailourines, *Simbakubwa* has deep carnassial notches on the molars and tall paracones fused to shorter metacones forming single piercing cusps. A Bayesian phylogenetic analysis recovers *Simbakubwa* as the sister taxon of a clade of large-bodied Miocene hyainailourines that includes *Hyainailouros* and *Megistotherium*. Bayesian ancestral state reconstruction supports an Afro-Arabian origin for Hyainailourinae with subsequent dispersal to Eurasia during the early Miocene. Regression analysis based on carnassial size is applied to *Simbakubwa* and closely related hyainailourines, recovering a body mass up to 1,500 kg for the new taxon. The evolution and extinction of Hyainailourinae offers important insights for interpreting ecological transitions from Paleogene to Neogene faunas in Afro-Arabia and Eurasia.

<http://zoobank.org/urn:lsid:zoobank.org:pub:3FB3BEB0-B0F8-4C65-97B1-7193CD071011>

SUPPLEMENTAL DATA—Supplemental materials are available for this article for free at www.tandfonline.com/UJVP

Citation for this article: Borths, M. R., and N. J. Stevens. 2019. *Simbakubwa kutokaafrika*, gen. et sp. nov. (Hyainailourinae, Hyaenodonta, 'Creodonta,' Mammalia), a gigantic carnivore from the earliest Miocene of Kenya. *Journal of Vertebrate Paleontology*. DOI: 10.1080/02724634.2019.1570222.

INTRODUCTION

Hyainailourine hyaenodonts are some of the largest terrestrial carnivorous mammals ever known (Savage, 1973; Ginsburg, 1980; Lewis and Morlo, 2010; Solé et al., 2015). Hyainailourinae likely originated in the early Paleogene (Borths et al., 2016) then dispersed across four continents, occupying apex carnivore niches in the Paleogene of Europe (e.g., *Kerberos*; Solé et al., 2015), Asia (e.g., *Orienspteron*; Egi et al., 2007), North America (e.g., *Hemipsalodon*; Mellett, 1969), and Afro-Arabia (e.g., 'Pterodon' *africanus*; Andrews, 1904). But it was not until the Miocene that evidence of the largest of the hyainailourines appeared, some approaching the size of rhinoceroses (Savage, 1973; Ginsburg, 1980; Morales and Pickford, 2017). These gigantic hyainailourines persisted well into the Neogene (Ginsburg, 1980; Barry, 1988), becoming part of Afro-Arabian and Eurasian ecosystems as other lineages of hyaenodonts declined and were ecologically replaced by carnivorans (Solé et al., 2015; Borths and Stevens, 2017a).

Hyainailourines generally differ from Carnivora in having three sets of carnassial blades, located between P4 and m1, M1 and m2, and M2 and m3 (Polly, 1996; Gunnell, 1998; Rose, 2006). Hyainailourines can be distinguished from other hyaenodonts in exhibiting hypercarnivorous dentition (sensu

Van Valkenburgh, 2007) with reduced talonids, absent metacoids, and tall paracones fused to shearing metacones (Borths et al., 2016). Hyainailourines persisted across the Paleogene-Neogene boundary in Afro-Arabia and at least one of the Afro-Arabian hyainailourine lineages dispersed to Eurasia during the Neogene (Ginsburg, 1980; Morlo et al., 2007; Sen, 2013) before going extinct in the late Miocene (Barry, 1980). The evolution and extinction of this radiation of hypercarnivores offers important insights into changing African terrestrial ecosystems through an interval of profound climatic (Zachos et al., 2001) and faunal (Stevens et al., 2013) changes.

Unfortunately, phylogenetic relationships among Miocene hyainailourines have been difficult to unravel given the fragmentary nature of much of the hyainailourine fossil record (Morales et al., 2003, 2007; Lewis and Morlo, 2010). The genus *Hyainailouros*, named by Biedermann (1863), has served as somewhat of a wastebasket taxon for many large but often fragmentary dental and postcranial remains recovered from early to middle Miocene sites across Eurasia and Africa (Pilgrim, 1932; Ginsburg, 1980; Lewis and Morlo, 2010). Similarly, *Isohyaenodon* and *Metapterodon* have served as repositories for small- to medium-sized Miocene hyainailourine fossils (Holroyd, 1999; Lewis and Morlo, 2010; Morales and Pickford, 2017). To complicate matters further, some fossils are missing dentition altogether, such as the massive early Miocene *Megistotherium* (Savage, 1973), making anatomical comparisons across taxa particularly challenging. As a result, unraveling the phylogenetic relationships among Miocene hyainailourines requires the discovery and

*Corresponding author.

description of well-preserved specimens that associate both dental and cranial features.

Here, we present a new hyainailourine from the Miocene of southwestern Kenya that is an important reference specimen for exploring the evolution of this clade. The material was discovered at the early Miocene Meswa Bridge locality, a site considered among the oldest early Miocene fossil localities in western Kenya based on faunal correlations with other radio-metrically dated fossil localities in the Songhor-Koru-Muhoroni area (e.g., Pickford, 1984). The Meswa Bridge locality also preserves hominoid, proboscidean, anthracothere, macroselidean, bird, and gastropod fossils (Pickford and Tassy, 1980; Andrews et al., 1981; Tassy and Pickford, 1983; Pickford, 1984; Harrison and Andrews, 2009; Werdelin, 2010) in addition to the hyainailourine described herein.

We refer to the new taxon a dentary that preserves a large canine, p4, and m3; a partial maxilla preserving P4, M1, and M2; several isolated teeth; an isolated calcaneum; and ungual phalanges. The holotype dentition is very lightly worn, and we refer all dental material to a single individual that died relatively early in adulthood (individual Dental Age Stage 3 in Anders et al., 2011). Unworn tooth crowns provide an opportunity to examine the dental anatomy of a group typically known from more fragmentary and heavily worn material (Savage, 1965; Ginsburg, 1980; Morales and Pickford, 2017). This dental material also offers an opportunity to estimate body mass for the new taxon, an essential data point for understanding the biology of the oldest gigantic hyainailourine in Afro-Arabia. We integrate the material into a Bayesian phylogenetic analysis that contextualizes hyainailourine evolution within the global radiation of Hyaenodonta. Results of the phylogenetic analyses are used as the basis of a biogeographic analysis of the Hyaenodonta and Hyainailourinae, tracking hyainailourines across continents from the Paleogene into the Neogene. Finally, we consider the biological differences between hyainailourines and the carnivorans that replaced them, offering avenues for further investigation into the carnivore transition that occurred through the early Neogene in Afro-Arabia and Eurasia.

Institutional Abbreviations—AMNH, American Museum of Natural History, New York, New York, U.S.A.; DPC, Duke Primate Center, Division of Fossil Primates, Duke University, Durham, North Carolina, U.S.A.; GSI, Geological Survey of India, Kolkata, India; GSN, Geological Survey of Namibia, Windhoek, Namibia; GSP-Y, Geological Survey of Pakistan, Islamabad, Pakistan; KNM, Nairobi National Museum, National Museums of Kenya, Nairobi, Kenya; LACM, Natural History Museum of Los Angeles County, Los Angeles, California, U.S.A.; MNHN, Muséum National d'Histoire Naturelle, Paris, France; NHMUK, Natural History Museum, London, United Kingdom; OCO, Orrorin Community Organisation, Kipsaraman, Baringo County, Kenya.

MATERIALS AND METHODS

Permissions

Materials described herein were examined at the Nairobi National Museum, National Museums of Kenya, under research permits issued by the Kenyan National Commission for Science, Technology and Innovation, with the authors as research affiliates of the National Museums of Kenya. GSP-Y specimens were studied while on loan to the Peabody Museum at Harvard University, Cambridge, Massachusetts, U.S.A.

Morphological Measurements and Nomenclature

Measurements were collected from digital photographs of the specimens using ImageJ (Schneider et al., 2012). Measurements

and dental nomenclature follow the definitions illustrated by Holroyd (1999) and Borths et al. (2016).

Body Mass Estimation

Body mass was estimated using three different regression equations that have been applied to the dentition of hyaenodonts. The regression equation employed by Morlo (1999) uses average lower molar length to predict body mass and was also used by Solé et al. (2015) to estimate the body mass of the large Eocene hyainailourine *Kerberos*. Van Valkenburgh (1990) described regression equations for estimating body mass in carnivores in different body size classes and different clades based on m1 length. We follow Friscia and Van Valkenburgh (2010) in using m3 in Hyaenodonta to estimate body mass. Because hyainailourines are hypercarnivores (sensu Holliday and Steppan, 2004), we use the Van Valkenburgh (1990) equation for Felidae, a clade with similar carnassial morphology. We also use the Van Valkenburgh (1990) equation for Carnivora greater than 100 kg. Many of the hyainailourines discussed in this study have larger carnassials than any living species in Carnivora. As a result, we are extrapolating body mass for these taxa beyond living models and outside of the clade from which the regression equations were derived. We present estimated body masses for these taxa to inform paleoecological discussion of giant hyaenodonts, although the current models available can only provide broad estimates for the masses of these extinct hypercarnivores.

Photogrammetry

Digital three-dimensional (3D) models of the holotype and referred specimens were generated using digital photographs collected with a digital single-lens reflex (DSLR) camera and the photogrammetry program Agisoft PhotoScan standard edition v. 1.3.4. The resulting photogrammetry models are accessioned in Morphosource (www.morphosource.org/) as Project 483.

SYSTEMATIC PALEONTOLOGY

MAMMALIA Linnaeus, 1758

EUTHERIA Huxley, 1880

HYAENODONTA Van Valen, 1967, sensu Solé et al., 2015

HYAINAILOUROIDEA Pilgrim, 1932, sensu Borths et al., 2016

HYAINAILOURINAE Pilgrim, 1932, sensu Solé et al., 2015

Emended Diagnosis—Emended after Solé et al. (2015). Hyainailouroids with buccolingually compressed, tall molar postpara-cristids and preprotocristids that intersect at near perpendicular angles; paraconid low and lingually positioned relative to protoconid; protoconid and paraconid subequal in mesiodistal length; all molar talonids reduced and open lingually; m3 talonid more reduced than m1 and m2 talonids; prominent anterior keel on m1–m3; paracone on M1 and M2 taller than metacone; M1 and M2 protocones low; P3 and P4 lingual cingula weak; rostrum constricted mediolaterally at P2; reduced postorbital process; dorso-ventrally deep zygomatic arch; choanae open proximate to M3; and circular subarcuate fossa on petrosal.

Note on Diagnosis—The diagnosis has been expanded relative to Solé et al. (2015) to include upper molar diagnostics that refer to the relative heights of molar paracones and metacones and lower molar diagnostics that describe the precise relationship between the paraconid and the protoconid.

Note on Taxonomy—We follow the taxonomic hierarchy of Hyaenodonta utilized by Solé et al. (2014, 2015), Rana et al. (2015), and Borths et al. (2016). An alternative is presented by Morales and Pickford (2017), which employs tribe-level taxa

that are broadly consistent with previously defined subfamily-level taxa (e.g., Hyainailourini in Morales and Pickford, 2017, is equivalent to Hyainailourinae in Rana et al., 2015).

SIMBAKUBWA KUTOKAAFRICA, gen. et sp. nov.
(Figs. 1A–C, 2–4, 5A, 6A, 7A, B, 8A–H)

Etymology—*Simbakubwa*, from Swahili ‘simba’ meaning ‘lion’ and ‘kubwa’ meaning ‘big’; *kutokaafrika*, from Swahili meaning ‘from Africa.’

Holotype—KNM-ME 20A, left dentary with canine, p4, m3, and alveoli of p3, m1, and m2 (dentary is reconstructed with the distal portion medially oriented out of natural position).

Paratypes—KNM-ME 20B, right rostral fragment with canine (plastered inaccurately), P3 alveoli, P4–M2; KNM-ME 20AI, left M2; KNM-ME 12, right lower canine; KNM-ME 23, right m1; KNM-ME 22, right m2; KNM-ME 13, left m2; KNM-ME 20P, left calcaneum; KNM-ME 20 AG, ungual phalanx; KNM-ME 20 AH, ungual phalanx.

Note: We hypothesize that the holotype and paratypes belonged to a single individual based on similar wear across the dentition and the non-duplication of any tooth or postcranial position. However, the material was excavated decades ago and thorough documentation is not associated with the material. We are taking a conservative path by designating the dentary specimen as the holotype, although it is likely the material belonged to a single subadult.

Additional postcranial material has been referred to this individual in the past, and the specimen number KNM-ME 20 applied to this material, with letter codes applied to each individual element. Other researchers have observed these specimens. The KNM has elected to preserve the existing specimen number and letter codes. Notes in the collection emphasize to researchers that every specimen originally labeled KNM-ME 20 is not necessarily referred to *Simbakubwa*. See Description and Comparisons and Supplemental Data 1 for evaluation of this postcranial material.

Type Locality—Muhoroni Agglomerates, Meswa Bridge, Kenya (Andrews et al., 1981).

Diagnosis—Differs from *Hyainailouros* in exhibiting molar protocones that project lingually rather than mesially; M2 parastyle bears multiple cusps; M1 and M2 metastyles more gracile; p4 mesiodistally shorter and buccolingually compressed; p4 talonid bears a single, buccolingually compressed cusp; m1 is mesiodistally longer relative to m2 and m3; and m2 and m3 postprotocristids slope steeply to carnassial notch. Differs from specimens referred to *Megistotherium* in having more buccolingually compressed trigonids relative to mesiodistal length on p4–m3; shallower mandibular corpus inferior to molar row; only two p3 alveoli; buccolingually compressed distal canine at alveolar margin rather than rounded; and m1 mesiodistally longer relative to m2 and m3. Differs from Fayum *Pterodon* by having mesiodistally short, buccolingually compressed talonids on m1–m3; and postprotocristid crests on m2–m3. Differs from *Pterodon*, *Orienspteron*, *Kerberos*, and *Hemipsalodon* by having more elongate metastyles on M1 and M2; mesiodistally shorter m3 talonid; and more buccolingually compressed canine.

DESCRIPTION AND COMPARISONS

Dentary and Lower Dentition

The left dentary (Fig. 1) preserves the canine, p4, and m3. The extent of the mandibular symphysis is difficult to determine given the reconstruction of the distal dentary. The coronoid process rises from a point immediately distal to m3 at a low angle (~150° relative to the horizontal ramus) and appears low and rounded, with a slight recurve along the posterior edge. The

morphology of the coronoid should be interpreted cautiously because it is reconstructed. The masseteric fossa is defined anteriorly by a broad coronoid ridge and inferiorly by a low, poorly defined ridge. The mandibular corpus is narrow, less than two times the height of m3 inferior to that tooth. The inferior margin of the mandible exhibits a convex curve inferior to the coronoid process. Medially, the insertion for the pterygoids is well defined near the inferior margin of the posterior end of the mandible. Mandibular foramina are preserved, but their position in relation to the teeth is difficult to determine based on the fragmentary nature of the jaw.

The lower canine (Figs. 1, 2) is buccolingually compressed, with a distinct distal cristid and a mesial groove that runs from the apex of the tooth to the alveolar margin, with crenulated enamel between this groove and the cristid. As is the case for other dental specimens referred to *Simbakubwa* in this study, the canine specimens are remarkably unworn. Measurements of the lower dentition are provided in Table 1.

On the two-rooted p4 (Fig. 1), there is no suggestion of a paraconid or a mesial cusp of any kind. The preprotocristid is distally inclined to the apex of the protoconid. The protoconid is the most prominent cusp. The postprotocristid is compressed into a distinct blade-like ridge that slopes steeply—nearly vertically—to the cristid obliqua, where it forms a distinct notch with the hypoconid. The hypoconid is the only cusp on the talonid, and it is buccolingually compressed into an apically rounded but shearing cusp. There is no suggestion of a talonid basin and no cingulids evident around the base of the tooth.

The m1 (Fig. 2) bears distinct paraconid, protoconid, and hypoconid. The apices of the paraconid and protoconid are lightly worn. The paraconid is lower than the protoconid and mesiolingually oriented relative to the protoconid, making the trend of the carnassial surface oblique to the mesiodistal axis of the tooth. The mesiobuccal face of the paraconid bears a distinct buccal keel, and the distal portion of the paraconid is compressed into a blade-like postparacristid that meets the preprotocristid in a deep carnassial notch. The protoconid is buccolingually compressed, with an elliptical cross-section and a blade-like preprotocristid. The postprotocristid slopes steeply to the cristid obliqua where it forms a distinct notch at the junction with the hypoconid. The hypoconid is buccolingually inflated and approximately one-third the height of the protoconid. The talonid basin is shallow and slopes gently lingually. The buccal aspect of the hypoconid also forms a shallow depression that slopes buccally, resulting in a broad base for the narrow blade of the hypoconid.

The m2 (Fig. 2) is 1.5 times the length of m1 (Fig. 2), consistent with the size difference inferred from the alveoli in the left dentary (Fig. 1). The paraconid and protoconid on m2 are taller than any of the cusps on m1. The enamel on m2 is crenulated on both the buccal and lingual faces of the paraconid, protoconid, and talonid. Like m1, the protoconid is the tallest cusp on m2. The paraconid is more mesially oriented on m2 than on m1, and the buccal keel is better defined. The paraconid is buccolingually compressed with an elliptical cross-section. The postparacristid tapers into a trenchant shearing blade that frames a deep carnassial notch with the preprotocristid. Lingual to the carnassial notch is a shallow, lingual depression. The preprotocristid curves more gently distally than the postparacristid. The postprotocristid forms a deep notch with the cristid obliqua, which descends to a point half the height of the hypoconid. Compared with the hypoconid of m1, the m2 hypoconid is more buccolingually compressed and the talonid basin is shallower and narrower. There is no suggestion of any other talonid cusp. The protoconid is mesiodistally longer than the paraconid, and the hypoconid is a third of the mesiodistal length of the protoconid. On the buccal aspect of both the carnassial notch and the cristid obliqua, there are shallow buccal depressions.



FIGURE 1. *Simbakubwa kutokaafrika* mandible, with *Panthera leo* mandible for comparison. *Simbakubwa kutokaafrika*, KNM-ME 20A, holotype, left dentary bearing a lower canine, p4, the alveoli of m1 and m2, and the recently erupted m3 in **A**, lingual, **B**, buccal, and **C**, occlusal views. **D**, *P. leo*, LACM 51553, modern male dentary in buccal view, for comparison. Note that KNM-ME 20A is reconstructed with the posterior portion of the mandible angled medially out of natural position. Scale bar equals 5 cm.

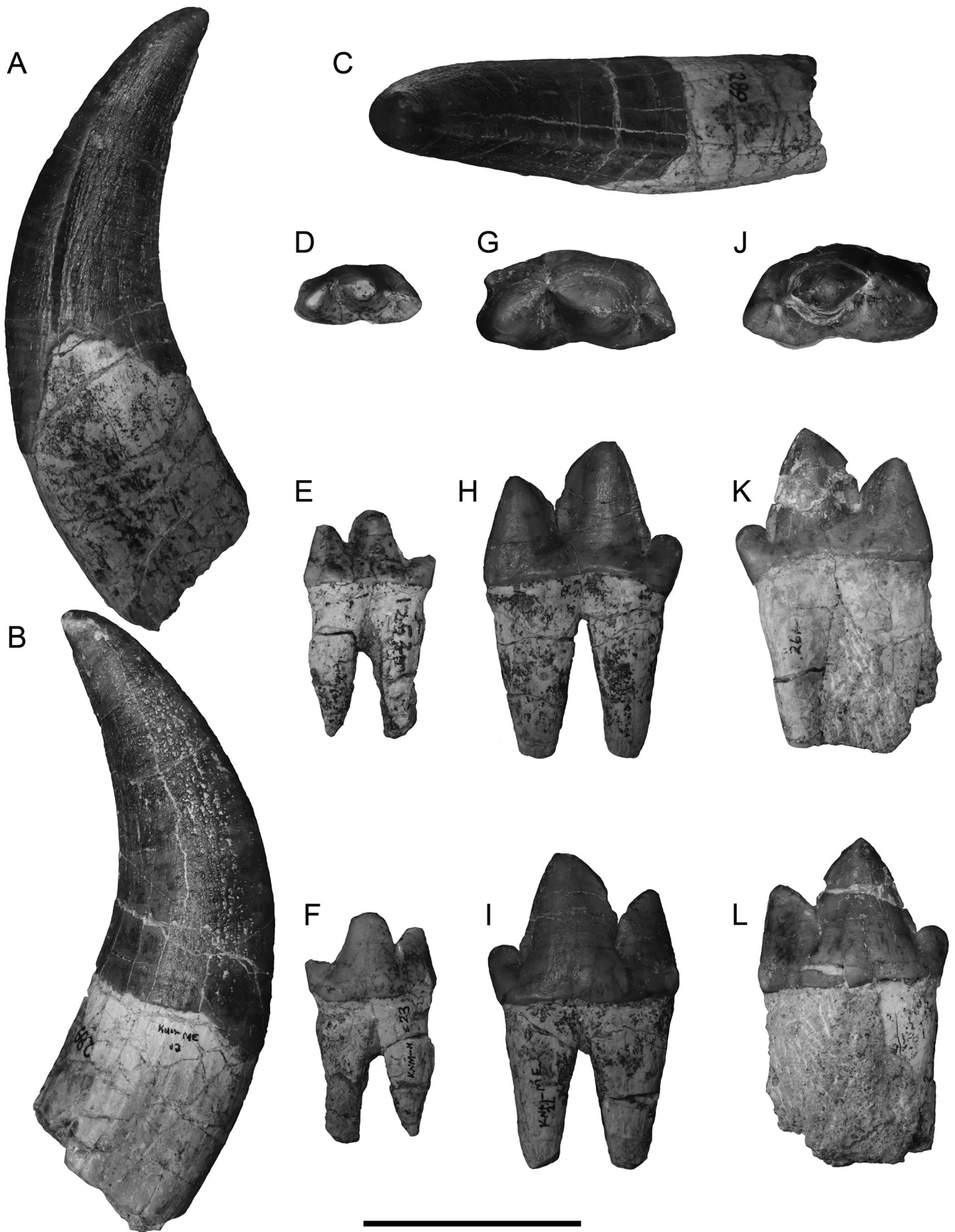


FIGURE 2. *Simbakubwa kutokaafrika*, isolated lower dentition. KNM-ME 12, right lower canine in **A**, lingual, **B**, buccal, and **C**, occlusal views. KNM-ME 23, right m1 in **D**, occlusal, **E**, lingual, and **F**, buccal views. KNM-ME 22, right m2 in **G**, occlusal, **H**, lingual, and **I**, buccal views. KNM-ME 13, left m2 in **J**, occlusal, **K**, lingual, and **L**, buccal views. Scale bar equals 5 cm.

TABLE 1. Lower dental measurements (in mm) of *Simbakubwa* and select hyainailourines.

Taxon	Specimen number	Locus	Total MD length	Trigonid MD length	Talonid MD length	Trigonid BL width	Talonid width	Talonid height
<i>Simbakubwa kutokaafrika</i>	KNM-ME 20A	Canine	42.5	—	—	27.8	—	—
		p4	33.4	26.1	7.8	21.8	9.1	12.9
		m1*	29.7	—	—	17.4	—	—
		m2*	45.4	—	—	24.6	—	—
		m3	56.4	54.8	2.1	26.9	6.4	6.6
	KNM-ME 12 KNM-ME 23 KNM-ME 22 KNM-ME 13	Canine	42.4	—	—	28.9	—	—
		m1	28.8	23.5	6.8	13.1	8.9	8.6
		m2	45.5	37.3	8.8	20	20.6	13.3
		M2	45.2	38.2	8.9	21.3	8.5	11.4
		p4	31.6	22.9	8.3	18.3	8.4	12.9
<i>Megistotherium osteothlastes</i>	DPC 6611, OCO BAR 109'03	m1	28.5	—	—	15.4	—	—
		m2	47.9 (1.3)	41.2 (3.0)	6.8 (1.7)	24.9 (0.6)	10.8 (4.7)	10.6 (0.9)
		m3	70	—	—	34.5	—	—
Arrisdrift hyainailourine	GSN AD 100'96	p3*	21.3	—	—	14.2	—	—
		dp4*	31.9	—	—	22.6	—	—
		m1	28.5	23.5	5.6	14.3	7.1	8.5
		m2*	41.5	—	—	22.3	—	—
		m3*	41.9*	—	—	17*	—	—
“ <i>Pterodon</i> ” <i>phiomensis</i>	AMNH 13253, AMNH 13254	p2	13.3 (0.4)	10.1 (0.4)	1.9 (0.1)	7.3 (0.4)	3.7 (0.4)	2
		p3	14.3 (0.1)	10.2 (0.2)	3.7 (0.6)	7.7 (0.1)	5.5 (0.6)	5.0 (1.1)
		p4	17.7 (0.2)	14.3 (0.8)	3.7 (0.7)	9.4 (0.5)	7.1 (0.2)	6.6 (0.6)
		m1	15.2 (2.3)	11.4 (1.0)	3.4 (0.9)	6.6 (1.1)	5.1 (1.2)	4.6
		m2	23.3 (0.2)	18.0 (0.1)	5.5 (0.5)	11.4 (0.7)	7.8 (0.6)	6.0 (0.5)
		m3	28.8 (3.9)	24.6 (3.3)	4.4 (1.1)	15.4 (1.0)	7.5 (1.6)	3.8 (2.5)
		m2	42.3	34	8.1	27.6	8.7	6.9
<i>Hyainailouros bugtiensis</i>	GSI D 107	m3	51.7	55.3	1.4	31.4	3.8	4.5
<i>Hyainailouros sulzeri</i>	MNHN.F.Or 311 and holotype	p3*	27	—	—	12	—	—
		p4	34.5 (0.8)	25.8 (1.1)	8.2 (1.3)	19.5 (1.1)	11.2 (0.5)	9.9 (4.1)
		m1*	27	—	—	19.3	—	—
		m2	43.5 (5.4)	33	7.4	21.2 (1.1)	9.8	11.3
		m3	51.6 (3.9)	47.3 (3.4)	4.9 (0.2)	26.1 (2.4)	8.8 (3.5)	11.3 (1.1)

Specimen details for hyainailourines included in Supplemental Data 1. **Abbreviations:** BL, buccolingual; MD, mesiodistal; *, measurements based on alveolar dimensions; **, measurement taken from worn dental material; —, morphology not preserved or not relevant to measurement.

The m3 (Fig. 1) is 1.25 times longer than m2. The paraconid is more mesially oriented than on m2 and is buccolingually compressed. The postparacristid forms a sharp blade, giving the paraconid a teardrop-shaped cross-section. The postparacristid and preprotocristid approximate each other at a point half the height of the paraconid, forming a parallel cristid arrangement that frames a deep carnassial notch that plunges close to the alveolar margin. The lingual face of the carnassial notch forms a deep, basin-like depression. The protoconid is buccolingually compressed, with a lenticular cross-section. The postprotocristid descends the distal face of the protoconid, subtly punctuated by a small bump near the alveolar margin, the only evidence of a talonid cusp.

Maxilla and Upper Dentition

A fragment of the right side of the rostrum (Fig. 3) preserves the canine, the alveoli of P3, and the crowns of P4, M1, and M2. There is a shallow embayment between the protocone of P4 and the protocone of M1, and a much deeper embayment between the protocones of M1 and M2. The buccolingually compressed canine is reconstructed out of natural position. The canine is unworn and relatively complete, with a teardrop-shaped cross-section formed by the distinct distal keel along the shearing edge of the tooth.

The P4 is ‘T’-shaped in occlusal view, with the tall, distally inclined paracone defining the intersection of the buccolingual and mesiodistal points of the tooth. The shelf-like parastyle is lower than the paracone and protocone, with a distinct enamel cingulum tracing the mesial face of the parastyle. Isolated from the parastyle, the protocone projects lingually and slightly

mesially relative to the paracone and the buccal margin. The protocone is low and rounded, sloping lingually, and lacking a distinct apex. The mesial and distal margins of the protocone are subparallel, and the distal margin of the protocone is weakly connected to the metastyle by a thin strip of enamel. The metastyle is a mesiodistally short cusp that is about two-thirds the length of the base of the paracone. The metastyle bears a sharp, buccolingually compressed metastylar blade that forms a distinct carnassial notch with the postparacrista. The buccal face of the carnassial notch exhibits a deep embayment, and a very narrow buccal cingulum runs from the distal-most point of the metastyle along the base of the metastyle, terminating at the carnassial notch. The metastyle of P4 contacts the mesial margin of M1 between the parastyle and the protocone. Measurements of the upper dentition are provided in Table 2.

The paracone is also the tallest cusp on M1 (Fig. 3) and is slightly inclined distally. The parastyle on M1 is taller and more prominent than the parastyle on P4. The parastyle bears a distinct primary cusp that is rimmed by several enamel crenulations along the buccal and mesial faces of the parastyle. The protocone is isolated from both the parastyle and the metastyle, with no indication of lingual cingula. The M1 protocone projects more mesially than the P4 protocone. The M1 protocone exhibits a distinct apex that is low and rounded, and the mesial and distal margins of the protocone parallel each other. The metacone is fused to the paracone, and its apex is only slightly lower than that of the paracone. The paracone and metacone can be distinguished by a deep trough dividing the cusps to their bases. The paracone cross-section is circular to ellipsoid, and the cross-section of the metacone is triangular, with a buccolingually



FIGURE 3. *Simbakubwa kutokaafrika*, KNM-ME 20B, right rostrum bearing upper canine, P3 alveoli, P4, M1, and M2 in **A**, lingual, **B**, buccal, and **C**, occlusal views. Scale bar equals 5 cm.

TABLE 2. Upper dental measurements (in mm) of *Simbakubwa* and select hyainailourines.

Taxon	Specimen number	Canine		P4		M1		M2	
		L	W	L	W	L	W	L	W
<i>Simbakubwa kutokaafrika</i>	KNM-ME 20B	40.5	26.4	30.1	22.7	46.1	30	52.4	40.7
	KNM-ME 20AI	—	—	—	—	—	—	48.8	38.1
<i>Megistotherium osteothlastes</i>	NHMUK PV M 26515 (right side)	53.1*	36.2*	34.9*	31.1*	40.7	34.2	47	36
<i>Hyainailouros napakensis</i>	Holotype	—	—	24.3	21	31.3	19.4	35	30
Arrisdrift hyainailourine	GSN AD 375'94	—	—	—	—	32.7	22.3	—	—
" <i>Pterodon</i> " <i>phiomensis</i>	AMNH 13251	—	—	21.3	14.7	23.5	14.6	28.5	20.8
<i>Leakitherium hiwegi</i>	NHMUK PV M 19083	—	—	—	—	16.6	15.7	15.8	13
<i>Hyainailouros bugtiensis</i>	GSP-Y 5884b	—	—	—	—	—	—	41.6	37.6
	GSP-Y 30940	—	—	35.3	30	44.4	33.2	52.8	41.1
<i>Hyainailouros sulzeri</i>	Holotype	—	—	28.1*	23.6	37.9	26.6	—	—
<i>Hyainailouros sulzeri</i>	NHMUK PV M 13999	—	—	—	—	—	—	42.4	31.7
<i>Hyainailouros sulzeri</i>	NHMUK PV M 14000	—	—	—	—	—	—	—	30.6

Abbreviations: L, mesiodistal length; W, buccolingual width; *, measurements based on alveolar dimensions.

compressed postmetacrista that forms a deep carnassial notch with the metastyle. The metastyle is a buccolingually compressed sectorial blade, with the mesiodistal extent equal to the mesiodistal length of the paracone and metacone bases. The metastyle rises from the carnassial notch, with a gentle convex curve that exhibits a slight concave inflection near the distal-most point of the metastyle. The lingual surface of the carnassial notch is a vertical face, and the buccal aspect of the carnassial notch is pinched into a deep depression. The distal point of the M1 metastyle contacts the mesiobuccal face of the M2 parastyle.

The lightly worn M2 (Figs. 3, 4) preserves complex morphology on the parastyle, with a prominent cusplule separated from a diminutive cusplule by an undulating enamel crest that terminates inferior to the apex of the primary cusplule. Enamel beading is formed along the distal aspect of the parastyle where it meets the base of the paracone. The protocone is lower than the buccal alveolar margin, and it bears a single, distinct, rounded cusplule. The protocone base is defined by a narrow lingual cingulum that is limited to the protocone. The protocone of M2 is more elongate and projects further lingually than the protocone of M1. The paracone and metacone on M2 are more fused than the condition in M1, with no distinct metacone apex. The metastyle of M2 is relatively taller than the metastyle of M1, and the

carnassial notch has a narrow slot bordered by the parallel blades of the postmetacrista and metastyle.

Craniodental Comparisons

Simbakubwa shares many features with hyainailourines, characteristics emphasized by Solé et al. (2015) and Borths et al. (2016). Like the Eocene hyainailourines *Kerberos langebaeae* (Solé et al., 2015), *Akhnatenavus nefertiticyon* (Borths et al., 2016), *Pterodon dasyuroides* (Lange-Badré, 1979), and *Hemipsalodon grandis* (Mellett, 1969), *Simbakubwa* exhibits a carnassial complex formed between upper molars that bear tall, piercing paracones that are nearly fused to lower, buccolingually compressed metacones and lower molars with obliquely oriented trigonids. The lower molars of each of these taxa lack a metaconid, and each talonid is relatively simple and shallow, with the most reduced talonid on m3.

During the early Miocene, there were large amphicyonid carnivorans such as *Amphicyon giganteus* (Ginsburg, 1980) and *Afrocyon burolleti* (Werdelin and Peigné, 2010) known from Libyan and Namibian faunas where they lived alongside large hyaenodonts (large amphicyonids are not yet known from eastern African faunas, but it is possible that they remain



FIGURE 4. *Simbakubwa kutokaafrika*, KNM-ME 20AI, M2 in A, occlusal, B, buccal, and C, lingual views. Scale bar equals 5 cm.

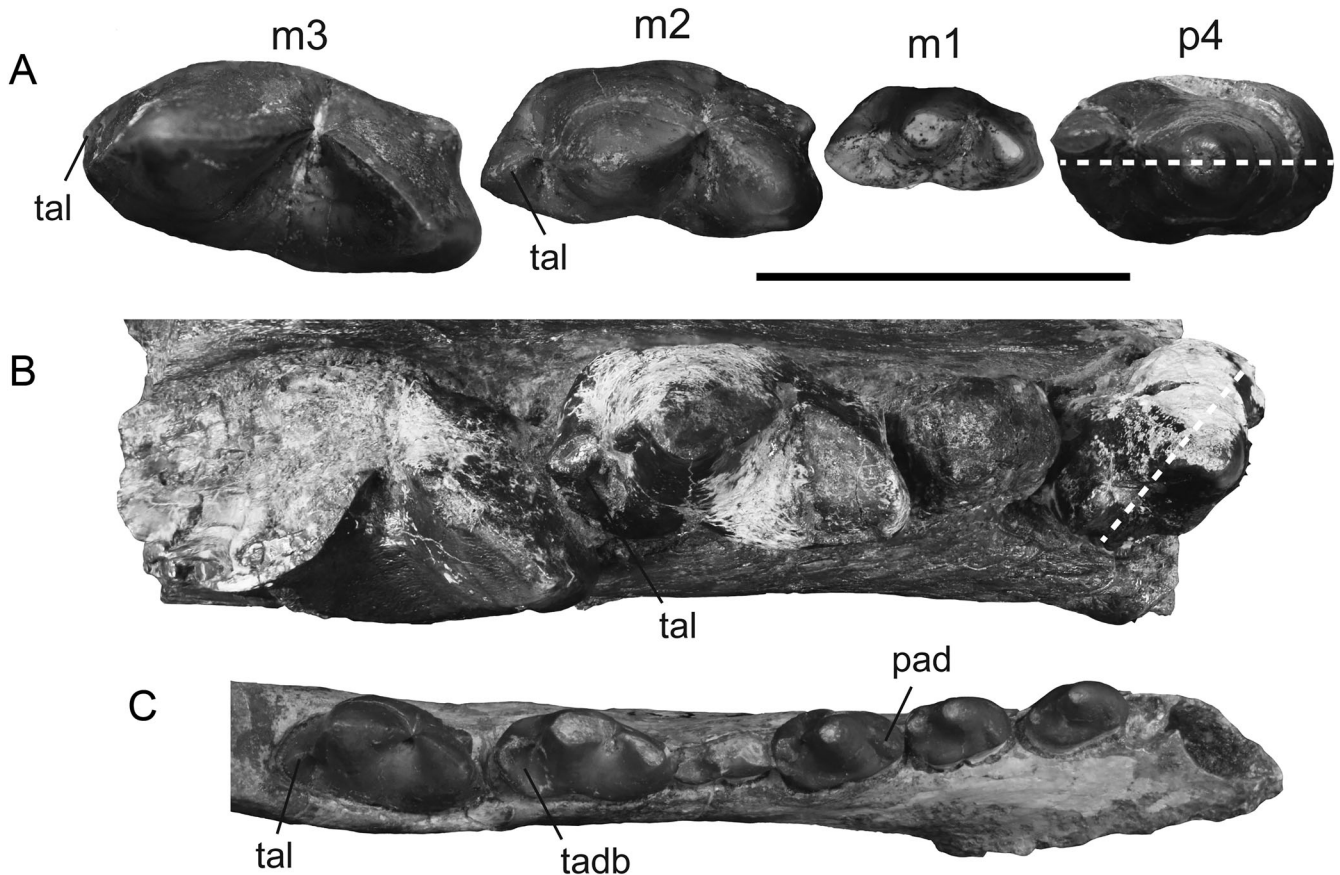


FIGURE 5. Lower dentition of *Simbakubwa kutokaafrika* compared with lower dentitions of large hyainailourines. **A**, composite lower tooth row of *Simbakubwa*, a hyainailourine from the lower Miocene of Kenya, composed of KNM-ME 20A (p4, m3), KNM-ME 23 (m1 reversed), and KNM-ME 22 (m2 reversed) in occlusal view. **B**, *Megistotherium osteothlastes* (reversed DPC 6611, p4–m3) from the middle Miocene of Egypt. **C**, ‘*Pterodon*’ *phiomensis* (reversed AMNH 13253, p2–m3) from the lower Oligocene of Egypt. The dashed line separates p4 talonid and paraconid. **Abbreviations:** pad, paraconid; tadb, talonid basin; tal, talonid. Scale bar equals 5 cm.

unsampled). A synapomorphy that separates carnivorans from hyaenodonts is the presence of only one pair of carnassials on each side of the skull formed between P4 and m1, a character that makes it relatively simple to distinguish the clades based on complete tooth rows. Isolated carnassials of large amphicyonids are distinguished from isolated carnassials of large hyainailourines by the presence of a single piercing paracone and an elongate metastyle on the upper carnassial and the presence of a metaconid and an expansive talonid on the lower carnassial of amphicyonids.

The hyainailourines most relevant for characterizing the morphology of *Simbakubwa*, a taxon from the earliest Miocene of eastern Afro-Arabia, are from the Oligocene through the middle Miocene of Afro-Arabia. ‘*Pterodon*’ *africanus* and ‘*Pterodon*’ *phiomensis* (Fig. 5) are the largest and best known of the Oligocene hyainailourines from the Fayum Depression, Egypt (Andrews, 1906; Schlosser, 1911; Holroyd, 1999; Borths et al., 2016). Note that these taxa are currently being reevaluated because *Pterodon* has been resolved as paraphyletic in recent works by Solé et al. (2015), Borths et al. (2016), and Borths and Stevens (2017a). *Simbakubwa* shares with ‘*P.*’ *africanus* a P3 with an expanded, but not individuated, distal root; a connate protocone on M1; a distally inclined paracone on P4 and M1; and an m1 that is close to the mesiodistal length of the trigonid of m2. *Simbakubwa* differs from ‘*P.*’ *africanus* and ‘*P.*’ *phiomensis* in its larger size, by exhibiting a

mesiodistally narrower P4 protocone and more expansive P4 parastyle, a buccolingually narrower M1 parastyle that does not buccally brace the metastyle of P4, a shallower buccal margin on M1 and M2 with only a slight ectoflexus, a mesiodistally wider and more lingually oriented M1 protocone, a p4 lacking a paraconid, a narrower m2 talonid basin, a more reduced m3 talonid, and a deeper m3 carnassial notch.

Geographically, the hyainailourine holotype found closest to *Simbakubwa* is *Hyainailouros napakensis* (Fig. 6). Found in the early Miocene (19–20 Ma; Werdelin, 2010) locality Napak I, Uganda, it was initially referred to *Pterodon africanus* by Savage (1965) then named *H. napakensis* by Ginsburg (1980). Morales and Pickford (2017), using a comparative figure in Rasmussen and Gutierrez (2009: fig. 14) of KNM-ME 22 (m2; Fig. 2) and KNM-LS 18230 (m3 protoconid; Rasmussen and Gutierrez 2009: fig. 14), suggested that the Losodok and Meswa Bridge material should be referred to *H. napakensis*. Based on the more complete material from Meswa Bridge that we refer to *Simbakubwa*, several distinctions can be observed that differentiate *Simbakubwa* from *H. napakensis* (the Losodok protoconid requires further examination in order to determine whether it should be referred to *Simbakubwa*). Compared with *H. napakensis* (Fig. 6), the Meswa Bridge material referred to *Simbakubwa* is larger and has a more individuated P4 protocone, a more lingually oriented M1 protocone, and buccolingually narrower and mesiodistally more elongate metastyles on M1

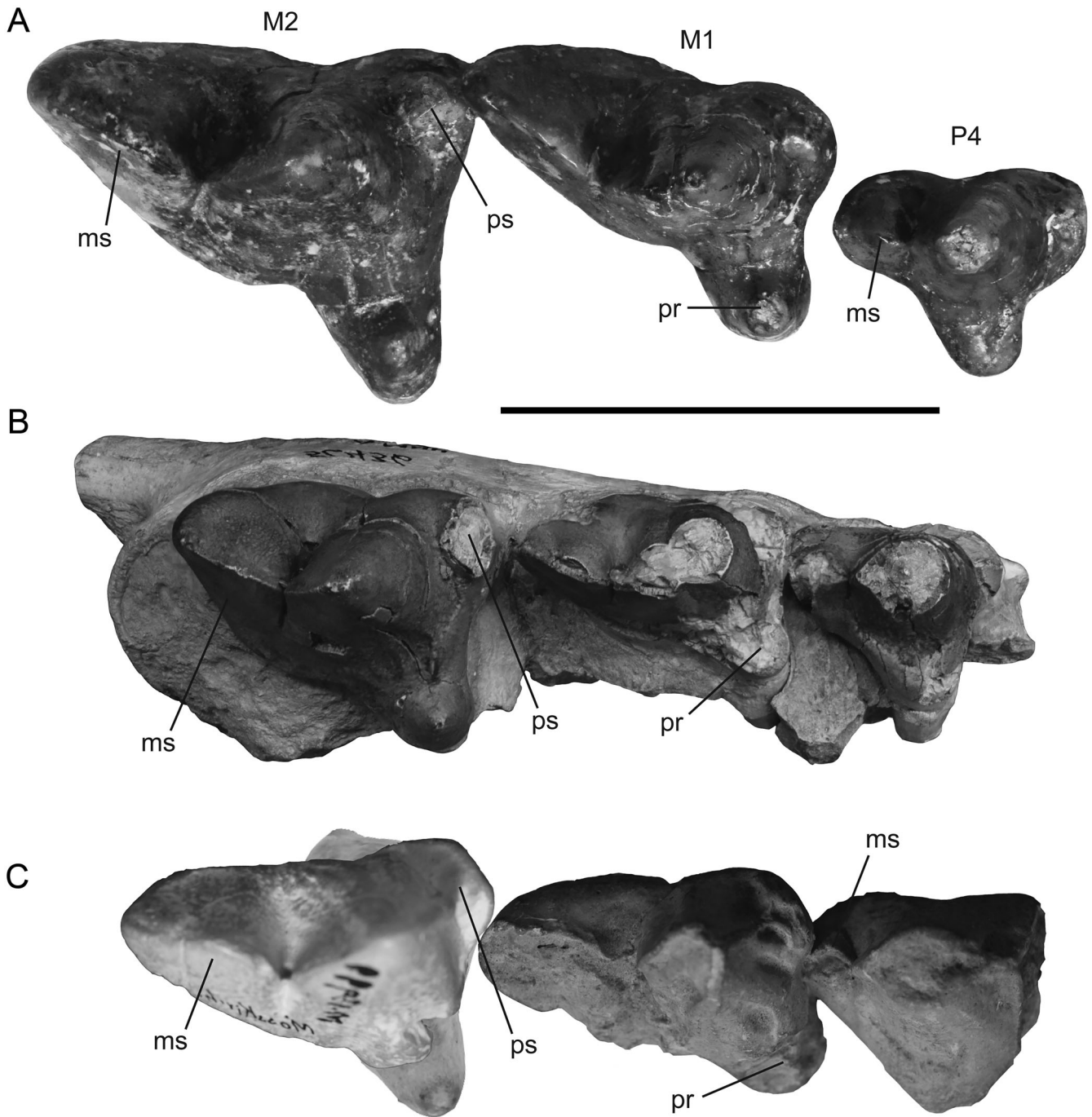


FIGURE 6. Upper dentition of *Simbakubwa kutokaafrika* compared with upper dentitions of large hyainailourines. **A**, P4, M1, and M2 of *Simbakubwa* from KNM-ME 20B in occlusal view. **B**, *Hyainailouros napakensis* (NHMUK PV M 19090, reversed) from the early Miocene of Uganda. **C**, *Hyainailouros sulzeri* from the middle Miocene of Europe (P4 and M1 from holotype, reversed; M2 composite of NHMUK PV M 13999 and NHMUK PV M 14000). Note the mesially shifted M1 protocone and robust M2 metastyle on *Hyainailouros*. **Abbreviations:** ms, metastyle; pr, protocone; ps, parastyle. Scale bar equals 5 cm.

and M2. The metastyles of *H. napakensis* are robust structures, with a wide alveolar base supporting the distal portion of the carnassial blade.

The robust metastyles on M1 and M2 and mesially shifted protoconids on M1 are also found in material referred to *Hyainailouros sulzeri* (Ginsburg, 1980), the type species of *Hyainailouros* from the middle Miocene of Europe (Fig. 6), and *Hyainailouros*

bugtiensis, a species from the middle Miocene of Pakistan and India (Pilgrim, 1912). Both are large hyainailourines, comparable in size to *Simbakubwa*. In addition to its gracile metastyles and lingually oriented protocones, *Simbakubwa* further differs from *H. sulzeri* in having multiple cusps along the rim of the parastyle of M2 and in exhibiting a single talonid cusp on p4 rather than multiple talonid cusps on p4 that surround a comparatively

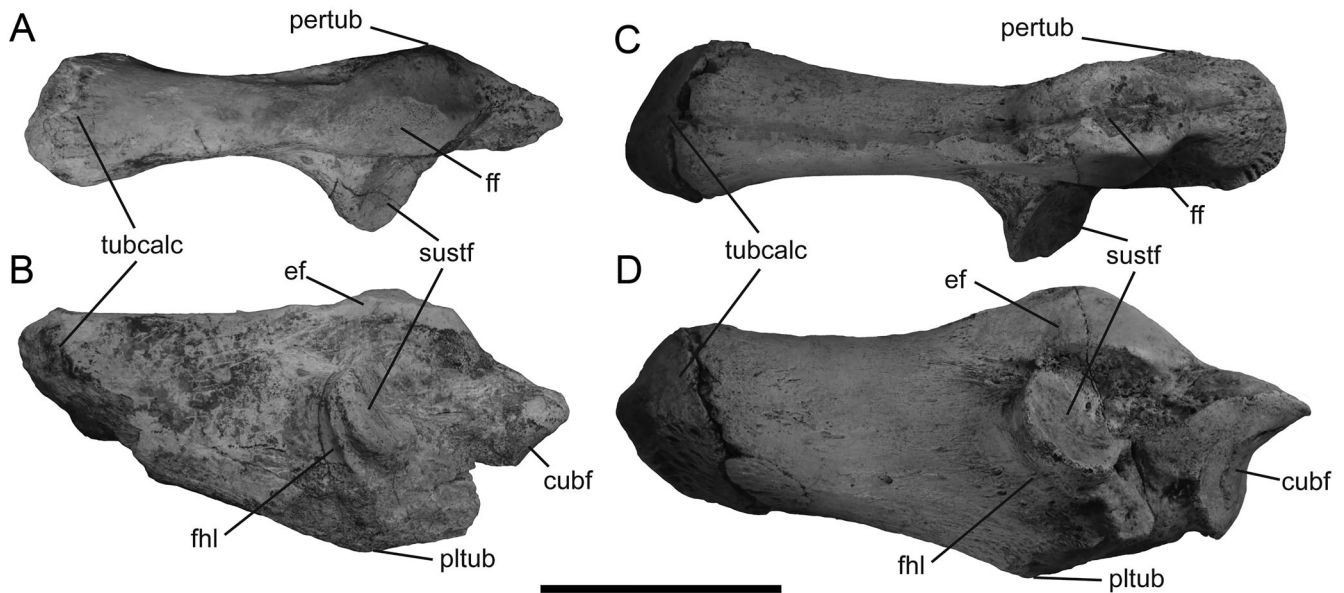


FIGURE 7. Calcaneum of *Simbakubwa kutokaafrika* compared with that of *Hyainailouros sulzeri*. KNM-ME 20P, left calcaneum referred to *Simbakubwa* in **A**, dorsal and **B**, medial views. MNHN.F.Or 311, right calcaneum (reversed) of *Hyainailouros sulzeri* in **C**, dorsal and **D**, medial views. **Abbreviations:** cubf, cuboid facet; ef, ectal facet; ff, fibular facet; fhl, groove for m. flexor hallucis longus; pertub, peroneal tubercle; pltub, plantar tubercle; sustf, sustentacular facet; tubcalc, tuber calcanei. Scale bar equals 5 cm.

broad talonid basin (Ginsburg, 1980:fig. 12). Both *Simbakubwa* and *Hyainailouros sulzeri* have very reduced m3 talonids that are essentially small bumps near the alveolar margin. The talonid of the m3 fragment referred to *Hyainailouros sulzeri* by Ginsburg (1980) has distinct enamel beading tracing the talonid onto the buccal face of the protoconid. The holotype of *H. bugtiensis* has a vertically oriented m3 postprocristid and an even more reduced talonid than is found on *Simbakubwa*.

Several specimens from Arrisdrift in the middle Miocene of Namibia have been referred to *H. sulzeri*; however, as noted by Morales et al. (1998), the M1 protocone (Morales et al., 1998:fig. 2) is more lingually directed and ‘horseshoe’-shaped than is observed in *Hyainailouros*, characters the Arrisdrift hyainailourine shares with *Simbakubwa*. The Arrisdrift hyainailourine differs from *Simbakubwa* in exhibiting a larger parastyle, taller metacone, and a rounded metastyle. Additional material from Arrisdrift, together with computed tomography (CT) scans of the juvenile hyainailourine dentary found at that locality, may help to further clarify the phylogenetic position of the Namibian taxon.

The holotype of *Megistotherium osteothlastes* is a gigantic, beautifully preserved cranium from the middle Miocene locality Gebel Zelten, Libya (Savage, 1965). Rasmussen et al. (1989) referred a dentary fragment from the middle Miocene locality Wadi Moghara, Egypt, to the species (Fig. 5). Although both specimens bear heavily worn and partially preserved dentition, enough morphology is present to differentiate *Megistotherium* from *Simbakubwa*. In *Simbakubwa*, P3 has two alveoli, with the distal alveolus buccolingually wider than the mesial alveolus, evidence that a slightly expanded cingulum-like protocone may have been present, like the protocone on P3 in *Pterodon africanus*. Three distinct roots supported P3 in *Megistotherium*. The diameter of the protocone alveolus in *Megistotherium* is as wide as the buccal alveoli. Based on the lingual alveolus of M1, *Megistotherium*, like *Hyainailouros*, had a mesially oriented protocone that stretched beyond the parastyle.

The p4 of *Megistotherium* is oriented obliquely relative to the molars. This distinctive morphology may have been shaped by a wide P3 protocone. In *Simbakubwa*, p4 is oriented along the mesiodistal axis formed by the lower molars. Both taxa share a simple, buccolingually compressed talonid with a single shearing hypoconid, rather than the complex talonid of *Hyainailouros sulzeri*. In *Megistotherium*, m1 is mesiodistally short. In most hyaenodonts, m1 is shorter than m2, but *Megistotherium* takes this trend to an extreme, with m1 barely the length of the m2 paraconid. In contrast, m1 in *Simbakubwa* is almost the length of the entire m2 trigonid. The trigonids of *Megistotherium* are buccolingually wider than the molar trigonids of *Simbakubwa*, and the talonid of m2 is mesiodistally shorter. Accompanying its robust lower molars, *Megistotherium* exhibits a far more robust dentary with a deep mandibular corpus relative to that of *Simbakubwa*, which is buccally inflected along the ventral margin. Solé et al. (2015) noted that dentary depth may reflect sexual dimorphism in some hyaenodonts, and the deep mandibular corpus of *Megistotherium* may reflect such intraspecific variation, although this is difficult to assess given the limited sample size for this taxon.

Postcrania

An isolated left calcaneum collected with the holotype of *Simbakubwa* (Fig. 7) shares much of the calcaneal morphology found on *Hyainailouros* (Fig. 7) and *Kerberos* (Solé et al., 2015), confirming its identity as hyainailourine, and we refer it to *Simbakubwa*. The calcaneum has a wedge-like tuber calcanei that appears to expand distally (note: a portion of the ventral and proximal surface is missing); a rounded, obliquely oriented sustentacular facet; a proximodistally elongate and medially facing ectal facet; a dorsally positioned fibular facet; and a cuboid facet that angles distally from the plantar to dorsal portion of the distal calcaneum. Relative to *Hyainailouros*, the sustentacular facet of *Simbakubwa* is more distally oriented; the groove for the tendon of flexor hallucis longus is directed toward the plantar tubercle and is more deeply

excavated; and the ectal facet is more medially oriented. Large amphicyonids were also present in the early Miocene of Africa (Werdelin and Peigné, 2010), but these caniform carnivorans have more obliquely oriented ectal facets and cuboid facets that are perpendicular to the long axis of the tuber calcanei (Argot, 2010).

Bifurcated ungual (distal) phalanges are a distinctive postcranial feature found in many hyaenodont taxa (Matthew, 1909; Mellett, 1977), including *Hyainailouros* (Ginsburg, 1980). Two ungual phalanges are associated with the holotype material of *Simbakubwa* (Fig. 8). Based on their size and the similarity to the bifurcated ungual phalanges referred to *H. sulzeri*, these specimens are referred to *Simbakubwa*. Each ungual phalanx has a mediolaterally broad tuberculum flexorium for the insertion of the tendon of the digital flexor and a wide margo coronalis around the base of the phalanx that supported the cuticle of the mediolaterally broad claw. On the axial and abaxial surfaces of the phalanges are large foramina soleare. The ungual phalanges are not referred to specific digits.

Comments on of Postcrania Referrals

Multiple postcranial elements were collected with the holotype of *Simbakubwa*, including a humerus, an ulna, a radius (Supplemental Data 1), a calcaneum (Fig. 7), and isolated ungual phalanges (Fig. 8). Given their large size, all of these elements were referred to the same specimen and were given the same accession prefix as the dental material (KNM-ME 20). Referring postcranial material to Afro-Arabian hyainailourines is difficult given the fragmentary fossil record of the group on the continent. Most taxa are known only from isolated dental elements. Savage (1973) referred a few postcranial elements, including a distal humerus and astragalus, to *Megistotherium*. Ginsburg (1980) questioned Savage's referrals in his description of a partial skeleton of *Hyainailouros sulzeri* from France. All specimens described by Ginsburg (1980) likely belonged to a single individual given the similar degree of epiphyseal fusion found across the skeleton and the light wear on all the fragmentary dental material. Ginsburg (1980) used the multiple associated elements of *H. sulzeri* to hypothesize that the humerus and astragalus originally referred to *Megistotherium* were more likely the remains of an amphicyonid such as *Amphicyon giganteus*. Ginsburg's (1980) work left no hyainailourines in the Miocene of Afro-Arabia with associated postcranial remains and made *Hyainailouros sulzeri* the most complete Miocene hyainailourine known.

Using forelimb material of *Hyainailouros sulzeri* as a reference, particularly the humerus, radius, and ulna (Supplemental Data 1), we do not refer the forelimb material collected at Meswa Bridge to *Simbakubwa*. The humeral material collected at Meswa Bridge (Supplemental Data 1) lacks a supratrochlear foramen and lacks a distinct medial epicondyle, both features found on the humerus of *Hyainailouros*. Further, the capitulum and trochlea on the Meswa Bridge humeri are not distinctly separated by a trochlear groove, a characteristic of the distal humerus of *Hyainailouros*. The cylindrical capitulum and deep olecranon fossa of the distal humeri from Meswa Bridge, the wide radial notch on the ulna, and the columnar radius indicate a forelimb incapable of supination or any appreciable degree of manual rotation. Exploration of the KNM collections reveals anthracothere postcrania also collected from Meswa Bridge. The forelimb material collected with the *Simbakubwa* holotype is remarkably similar to the anthracothere forelimb material collected from Meswa Bridge and Rusinga Island, Kenya (Supplemental Data 1). Anthracothere postcranial specimens from the Miocene of Afro-Arabia are also fragmentary and rarely associated with dental remains, but for reasons outlined above, at this time we tentatively refer forelimb postcranial

specimens collected with *Simbakubwa* to Anthracotheriidae rather than Hyainailourinae.

PHYLOGENETIC AND BIOGEOGRAPHIC ANALYSIS

Materials referred to *Simbakubwa* were placed into a phylogenetic context by expanding the character-taxon matrix published by Borths and Stevens (2017b) with new characters (character 2, dp3 protoconid; character 20, p4 orientation; character 37, m1 mesiodistal length; character 77, upper canine cross-section; character 88, metastyle robusticity) and modified character states directly informed by *Simbakubwa* morphology. This analysis includes 156 characters and 94 operational taxonomic units (OTUs). Nineteen of the characters were treated as ordered for this analysis. Descriptions of the characters, with ordered states and modifications relative to Borths and Stevens (2017b), and specimens used to code each OTU are included in Supplemental Data 1. The character-taxon matrix formatted for Mesquite (Maddison and Maddison, 2016) is Supplemental Data 2.

The matrix was analyzed using the Bayesian 'tip-dating' phylogenetic methods described by Beck and Lee (2014) and used to analyze hyaenodont systematics in previous studies (Borths et al., 2016; Borths and Seiffert, 2017; Borths and Stevens, 2017a, 2017b). This model-based method uses the character-taxon matrix and OTU age ranges to simultaneously estimate branch lengths, evolutionary rates, phylogeny, and support for each clade and is increasingly common for morphological analyses of paleontological data (for methodological discussion, see Beck and Lee, 2014; Dembo et al., 2015; Gorscak and O'Connor, 2016; Heritage et al., 2016; Lund et al., 2016; Sallam and Seiffert, 2016). The nexus file, analyzed using MrBayes (Ronquist et al., 2012), including all analytical parameters, is Supplemental Data 3. The clock rate prior used in the tip-dating analysis followed the methods described in Heritage et al. (2016) using the *dist.nodes* function from the R package APE (v. 3.4) (Paradis et al., 2004) and the *fitdist* function from the R package *fitdistrplus* (v. 1.0-6) (Delignette-Muller and Dutang, 2015). Justification of the age range for each OTU is included with specimen notes in Supplemental Data 1.

Results of the phylogenetic analysis and the biogeographic ancestral state reconstruction analysis are shown in Figure 9. The 'all-compact' consensus phylogeny with all OTUs and node statistics, including the median age range for the origin of each node, and evolutionary rates for each branch are presented in Supplemental Data 4 and can be viewed in the Nexus viewer FigTree (Rambaut, 2016). Summary statistics for the Bayesian phylogenetic analysis are included in Supplemental Data 5.

A model-based biogeographic analysis was conducted using the ancestral state reconstruction program RASP (Yu et al., 2015) with the analytical parameters described by Borths and Stevens (2017a). This study was conducted to generate a reproducible framework for interpreting the dispersal patterns that led to the widespread distribution of Hyainailourinae during the middle Miocene. Previous examinations focused on hyainailourine biogeography (Ginsburg, 1980; Gheerbrant and Rage, 2006; Solé et al., 2015) have used phylogenies to inform biogeographic reconstructions, but these were not model based. We test for dispersal rather than vicariance events using Bayesian binary Markov chain Monte Carlo (BBM) ancestral state reconstruction on the consensus tree recovered from the Bayesian 'tip-dating' analysis. The results of the ancestral state reconstruction analysis are visualized in Figure 9, and results for each node can be viewed individually in RASP by loading Supplemental Data 6.

The results of the phylogenetic analysis and biogeographic ancestral state reconstruction are discussed together. No standardized framework has been developed for discussing posterior probability (PP) support, but we follow Borths et al. (2016) in defining PP support less than 50% as 'weak.' The phylogenetic analysis

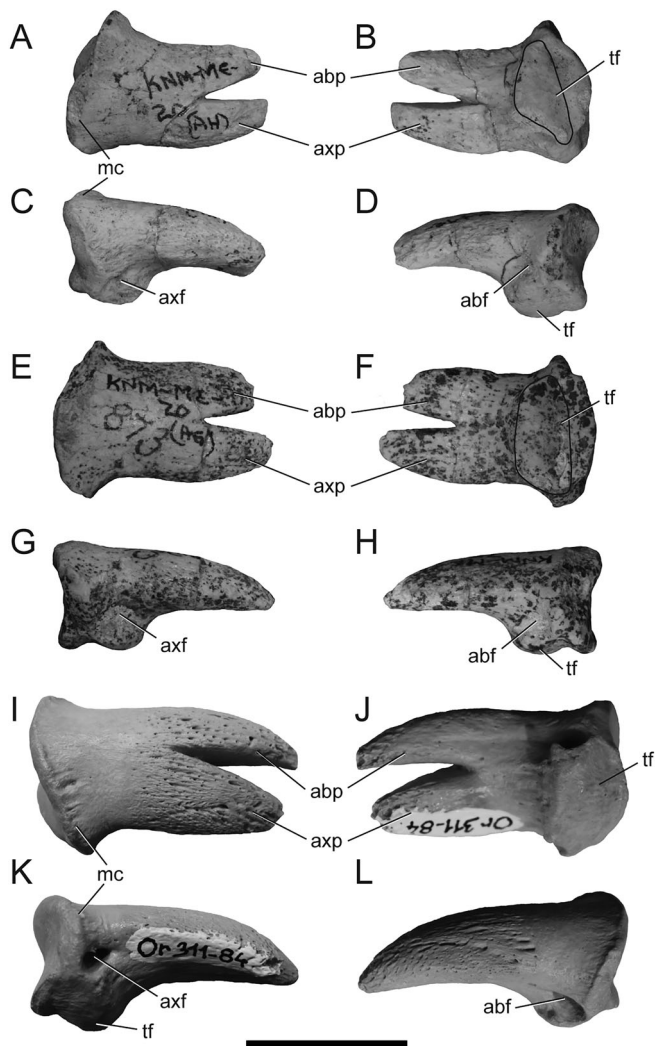


FIGURE 8. Ungual phalanges of *Simbakubwa kutokaafrika* compared with those of *Hyainailouros sulzeri*. KNM-ME 20AH, unguals of *S. kutokaafrika* in A, dorsal, B, plantar, C, axial, and D, abaxial views. KNM-ME 20AG, unguals of *S. kutokaafrika* in E, dorsal, F, plantar, G, axial, and H, abaxial views. MNHN.F.Or 311-84, unguals referred to *H. sulzeri* in I, dorsal, J, plantar, K, axial, and L, abaxial views. **Abbreviations:** abf, foramen soleare abaxiale; abp, processus unguicularis abaxialis; axf, foramen soleare axiale; axp, processus unguicularis axialis; mc, margo coronalis; tf, tuberculum flexorium. Scale bar equals 2 cm.

resolves *Simbakubwa* as the sister taxon of the clade that includes *Hyainailouros* with posterior probability (PP) support of 56%. The *Hyainailouros* clade is very weakly supported (PP = 15%), and it recovers *H. sulzeri* as the sister taxon of the Namibian hyainailourine and *H. napakensis* as the sister taxon of a clade that includes *Isohyaenodon andrewsi*, *H. bugtiensis*, and *Sivapterodon lahirii*. The *Simbakubwa* lineage likely diverged from the *Hyainailouros* clade during the Oligocene before *Hyainailouros* dispersed from Afro-Arabia to Europe (100% likelihood) in the early Miocene. Based on these results, *Sivapterodon* and *H. bugtiensis* represent a second dispersal of hyainailourines to Eurasia during the Miocene. *Falcatodon*, a taxon known from the early Oligocene of Egypt, is the sister taxon of the hyainailourine clade that includes *Simbakubwa*. *Megistotherium* is recovered as the sister taxon of *Leakitherium* and is nested within the sister clade of the *Falcatodon*, *Simbakubwa*, and *Hyainailouros*

clade. The weakly supported *Megistotherium* clade (PP = 20%) includes the rest of the Miocene hyainailourines: *Mlanyama*, *Metapterodon*, *Isohyaenodon zadoki*, and *Exiguodon*. The clade that includes all Miocene hyainailourines most likely originated in Afro-Arabia (100% likelihood given the phylogeny) in the latest Eocene.

The sister taxon of Hyainailourinae is Apterodontinae. These lineages most likely originated in Afro-Arabia and diverged from each other in the early middle Eocene. Hyainailourinae is weakly supported (PP = 33%) with *Orienspterodon* as the sister taxon of the clade that contains the rest of Hyainailourinae. During the middle Eocene, there were multiple hyainailourine dispersals from Afro-Arabia to Eurasia, including the dispersal of *Orienspterodon*, *Kerberos* + *Pterodon dasyuroides*, and *Paroxyaena*. There is evidence that the apterodontine lineage that includes *Apterodon gaudryi* dispersed to Europe during the early Oligocene, but there does not seem to be a comparable hyainailourine dispersal during this time. During the early Miocene, the teratodontine *Dissopsalis* dispersed from Afro-Arabia to southwestern Asia along with *Hyainailouros* and *Metapterodon*.

The hyaenodont clades and their biogeographic origins illustrated in Figure 9 are broadly consistent with similar analyses presented in Borths et al. (2016) and Borths and Stevens (2017a). The support for early branching nodes that reconstruct the relationships between North American hyaenodont clades such as *Galecyon* and *Pyrocyon* are exceptionally weak, evidence that these relationships are in need of further investigation.

BODY MASS ESTIMATION

The most striking feature of *Simbakubwa* is the size of the specimen. Based on its massive dentition, the animal was significantly larger than any modern African terrestrial carnivore. Body mass is one of the most biologically significant aspects of a carnivore's morphology (Gittleman, 1995; Carbone et al., 1999); hence, an estimation of the body mass of *Simbakubwa* is an important aspect of the role it played in the early Miocene ecosystem preserved at Meswa Bridge. Simple comparisons between the dentary of *Simbakubwa* and *Panthera leo* (Fig. 1) reveal that the Miocene carnivore was significantly larger than the modern lion.

Both Van Valkenburgh (1990) and Morlo (1999) have described equations that use carnassial molar length (m1 length) to estimate body mass in Carnivora, and both have modified these equations to reconstruct body mass in hyaenodonts. In order to apply a carnivoran regression equation to hyaenodonts, Morlo (1999) averaged the length of each hyaenodont carnassial in a single dentary. The body mass estimate produced for *Simbakubwa* using the Morlo (1999) equation is 1,308 kg, a mass larger than the largest living terrestrial carnivore *Ursus maritimus* (polar bear; Gunderson, 2009). Friscia and Van Valkenburgh (2010) proposed using m3 mesiodistal length rather than average molar length for estimating hyaenodont body mass from carnivoran-based regression equations. Using m3 length in the Felidae regression equation from Van Valkenburgh (1990), an equation derived from a clade of carnivores with similar carnassial morphology to Hyainailourinae, we predict a body mass of 1,554 kg in *Simbakubwa*. Using m3 length in the Van Valkenburgh (1990) equation for carnivorans greater than 100 kg, an equation derived from a sample that includes hyper- and hypocarnivores, we predict a body mass of 280 kg for *Simbakubwa*, placing it among the largest lions (Schaller, 1972).

Dental dimensions do not necessarily offer the most accurate estimates of body mass, as evidenced by the extensive range of estimates produced by different regression equations. Other studies have utilized cranial and postcranial dimensions

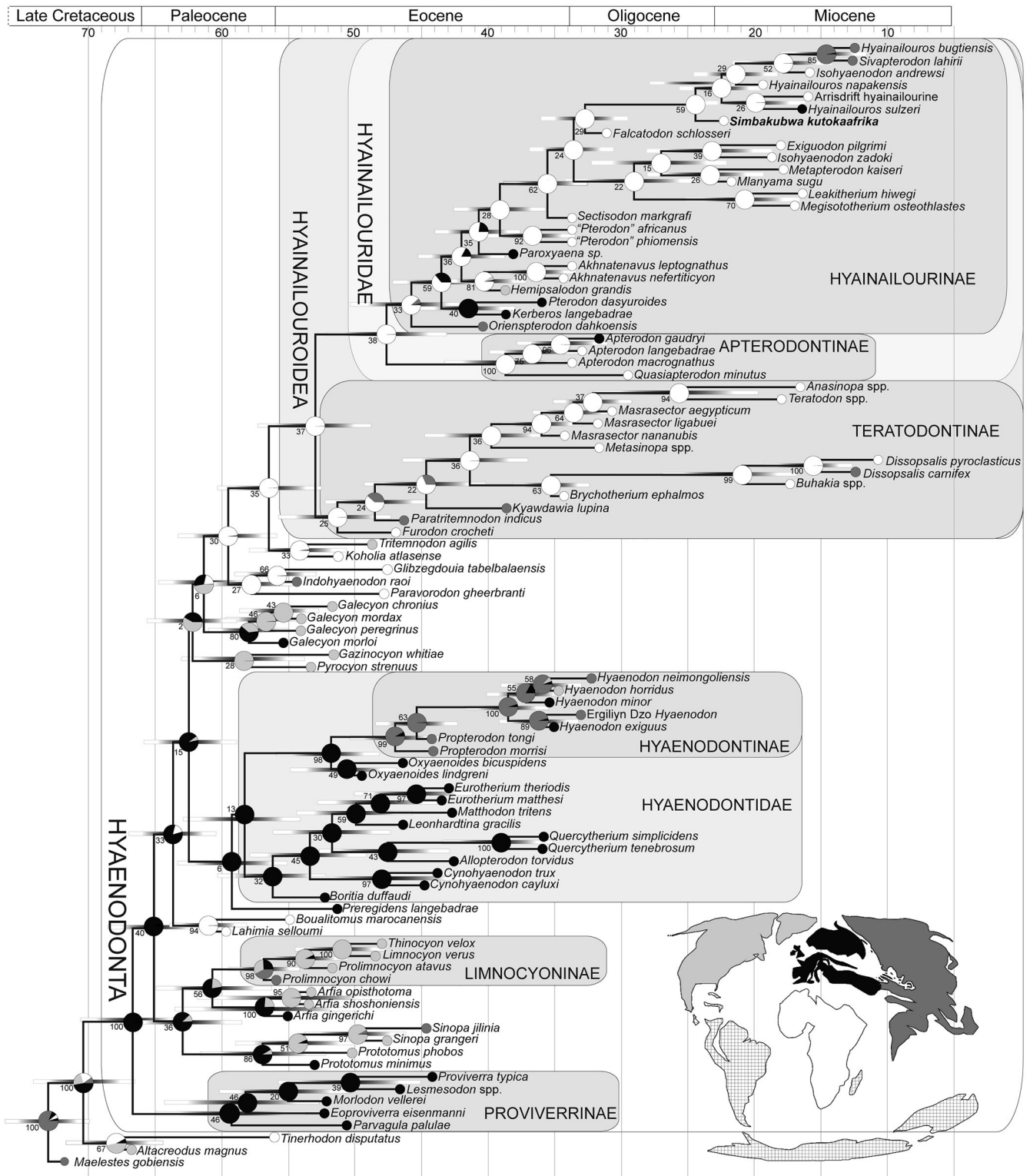


FIGURE 9. Phylogeny and biogeography of Hyainailourinae. Summarized results of the Bayesian 'tip-dating' analysis performed using 94 OTUs and 156 morphological characters illustrated using the 'allcompat' Bayesian consensus tree. Divergence dates and terminal ages reflect the median age estimate for the taxon or node. Pie charts indicate relative support for ancestral continental area for each node based on Bayesian binary MCMC (BBM) biogeographic analysis: Afro-Arabia in white; Europe in black; North America in light gray; Asia (including India) in dark gray; absence of hyaenodonts indicated by grid pattern. Terminal circles indicate continent where OTU was discovered. Posterior probability support shown left of relevant node. Nodal gradient bars represent 95% highest posterior density (HPD) age estimates. Evolutionary rate estimates and date ranges for each OTU are contained in Supplemental Data 4. BBM results for each node in Supplemental Data 6.

TABLE 3. Body mass estimates (in kg) for *Simbakubwa* and large hyainailourines.

Taxon	Morlo	VV1	VV2
<i>Simbakubwa kutokaafrika</i>	1308	1554	280
<i>Megistotherium osteothlastes</i>	1794	3002	317
<i>Hyainailouros bugtiensis</i>	1744	1192	267
<i>Hyainailouros sulzeri</i>	1276	1185	266
Arrisdrift hyainailourine	828	628	237
<i>Hyainailouros napakensis</i>	255*	271	202
<i>Pterodon phiomensis</i>	158	200	191

For taxa with multiple referred specimens, average length for all specimens was used for the regression. **Abbreviations:** **Morlo**, estimate based on Morlo (1999) for hyaenodonts using average mesiodistal length of carnassial-bearing molars; **VV1**, estimate based on Van Valkenburgh (1990) for Felidae; **VV2**, estimate based on Van Valkenburgh (1990) for Carnivora >100 kg; *, lower molar mesiodistal length inferred from upper dentition using methods described by Borths and Stevens (2017a).

to more accurately reconstruct body mass in meat-eating mammals (Van Valkenburgh, 1990; Egi, 2001; Sorkin, 2008). Estimates of hyainailourine body mass presented herein (Table 3) are based on the best available data for this important taxon, with the hope that the discovery of more complete material can further refine our understanding of the large-bodied hyainailourines.

DISCUSSION AND CONCLUSIONS

Biogeography of Hyainailourinae

Meswa Bridge is one of the oldest Neogene localities in sub-Saharan Africa (Werdelin, 2010). This makes *Simbakubwa* the oldest known member of the hyainailourine giants and a key taxon for understanding the dispersal of large hyainailourines to ecosystems on the northern continents. The middle Miocene was an interval of increasing tectonic and faunal connectivity between Afro-Arabia and Eurasia (Sen, 2013), and the direction of dispersals within Hyainailourinae is an important component for understanding larger patterns of accommodation and exchange between landmasses (Fig. 10).

The presence of *Simbakubwa* in the early Miocene supports the hypothesis advocated by Solé et al. (2015) and tested in this study that the large-bodied hyainailourines represent a distinct dispersal event from Afro-Arabia. Phylogenetic and biogeographic evidence supports a Eurasian origin for Hyaenodonta in the early Paleocene followed by rapid dispersal to Afro-Arabia and North America (Fig. 10A). Results suggest that Hyainailourinae originated in Afro-Arabia during the earliest Eocene, then hyainailourine lineages dispersed to Europe, Asia, and North America through the early and middle Eocene (Fig. 10B). By the middle Oligocene, hyainailourines appear to have become extinct on the northern continents but persisted in Afro-Arabia, giving rise to the clade that includes *Simbakubwa* and *Hyainailouros* (Fig. 10C). In the early Miocene or early late Oligocene, faunal exchange between Afro-Arabia and Eurasia was likely enabled by the appearance of the ‘*Gomphotheres*’ land bridge (Van der Made, 1999; Antoine et al., 2003), which facilitated the arrival of the *Gomphotheres* lineage and possibly the *Hyainailouros bugtiensis* lineage in Eurasia around 19.6 Ma and the arrival of the *Hyainailouros* lineage in Europe around 16.9 Ma (MN4; Rössner and Heissig, 1999). By the middle Miocene, Hyainailourinae were well established in Eurasia, with *Hyainailouros sulzeri* in Europe (Ginsburg, 1980) and *H. bugtiensis* and *Sivapterodon lahirii* in southwestern Asia (Pilgrim, 1932; Barry, 1988) (Fig. 10D). The phylogenetic and biogeographic evidence presented here for separate dispersal events during the Miocene

for the southwest Asian hyainailourines and the European hyainailourines is consistent with biogeographic hypotheses presented by Morlo et al. (2007). Hyainailourines continued to diversify in Afro-Arabia, giving rise to the groups that include *Megistotherium* (Savage, 1973; Rasmussen et al., 1989) and the middle Miocene Arrisdrift hyainailourine (Morales et al., 1998; Morales and Pickford, 2017). Hyaenodont lineages that include *Dissopsalis* (Barry, 1988) and *Metapterodon* cf. (Barry, 1980) likely also originated in Afro-Arabia and dispersed to Eurasia during the early Miocene, perhaps alongside the group containing *Hyainailouros bugtiensis*.

Carnivora appear to have dispersed in the opposite direction, moving from Eurasia into Afro-Arabia in the late Oligocene or earliest Neogene (~23 Ma). The timing of this dispersal is inferred both from fossils (Hooijer, 1963; Rasmussen and Gutierrez, 2009) and molecular evidence (Yoder et al., 2003). Borths and Stevens (2017a) summarized shifts in the carnivore fauna in Afro-Arabia in the early Neogene, with existing evidence suggesting that the earliest Afro-Arabian carnivores were relatively small mesocarnivores. As new taxa dispersed to Africa throughout the Miocene, Carnivora diversified phylogenetically and morphologically while the Afro-Arabian landscape underwent dramatic transformations, with the initiation of the East African Rift System in the late Oligocene (Roberts et al., 2012) followed by the continued uplift of eastern Afro-Arabia (Partridge, 2010), division of the Tethys seaway by the Arabian Peninsula, and transformation of forested environments into seasonally drier and more open habitats reflected by profound faunal shifts (Evans et al., 1981; Sepulchre et al., 2006; Stevens et al., 2013).

Simbakubwa would be a remarkably large taxon at any point in the Neogene, but its occurrence in the earliest Neogene makes it particularly fascinating as evidence of the adaptive response of hyaenodonts to the changing Afro-Arabian fauna and environment. *Simbakubwa* is larger than any Paleogene hyaenodont, including the largest early Oligocene Fayum hyaenodont ‘*Pterodon*’ *africanus*. The late Oligocene Afro-Arabian fossil record is sparse (Stevens et al., 2013), and it is possible that gigantic hyaenodonts were part of terrestrial faunas before the earliest Miocene, but *Simbakubwa* is definitive evidence that the earliest Neogene environments supported gigantic carnivores. Further, we suggest that a key factor that drove hyainailourines to sizes as large as *Simbakubwa* may simply have been changes in the herbivore fauna due to changes in the Afro-Arabian landscape (Sen, 2013), rather than hyainailourine-carnivoran competition, because carnivores did not diversify until later in the Miocene. After hyainailourines became gigantic, as exemplified by *Simbakubwa*, the conditions that supported this new hyaenodont morphology appear to have persisted through the Miocene. *Simbakubwa* is the earliest evidence of an ecomorphological experiment that succeeded in ecosystems on three continents for an interval spanning at least 15 million years. The presence of *Simbakubwa* and its large relatives in these ecosystems informs interpretations of carnivore faunal shifts over the Miocene (e.g., Pires et al., 2017) and brings into focus larger questions about the evolution of modern terrestrial ecosystems across Africa and Eurasia.

Paleoecology of *Simbakubwa*

The three basic ecomorphological features used by researchers interested in the evolution of hyaenodonts and carnivores are body size, dental morphology, and locomotor behavior (Morlo, 1999; Morlo et al., 2010; Friscia and Van Valkenburgh, 2010). The nearly pristine dental specimens referred to *Simbakubwa* reveal that at a size between 280 and 1,500 kg, this animal was a specialized hypercarnivore that was at least the size of the largest lions and possibly larger than a polar bear. Fewer specimens are available to reconstruct the locomotor guild occupied by *Simbakubwa* with any confidence, although the referred calcaneum

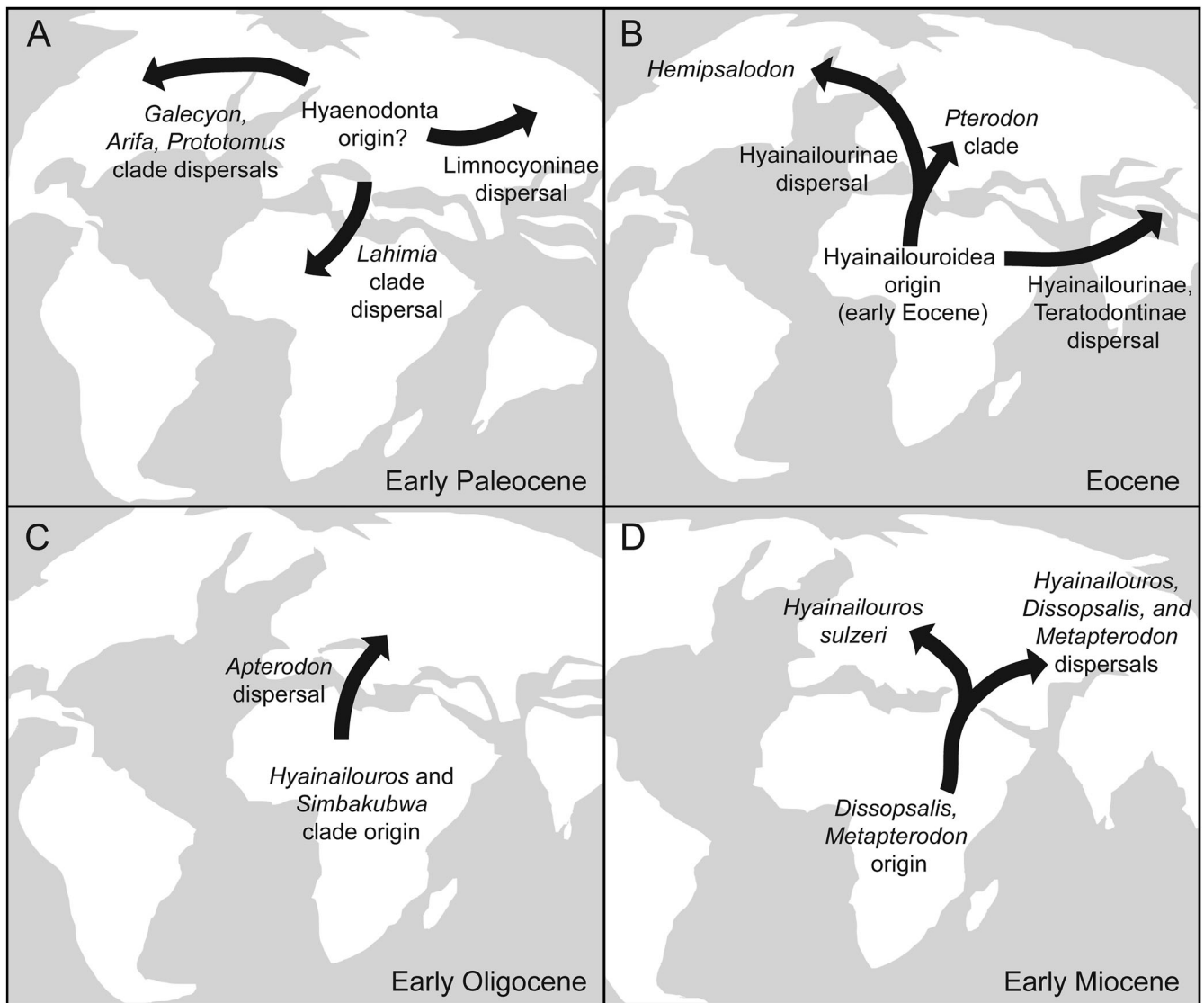


FIGURE 10. Biogeographic history of *Simbakubwa* and Hyainailourinae. Based on the Bayesian ancestral state reconstruction and the topology shown in Figure 9, Hyaenodonta most likely originated in Europe in the early Paleocene (A) and rapidly dispersed to Afro-Arabia, giving rise to the *Lahimia* clade, the oldest on the continent. Hyaenodonta diversified during the Eocene (B), appearing to give rise to endemic clades in North America, Europe, and Afro-Arabia. Reconstructions indicate that Hyainailouroidea originated in Afro-Arabia during the earliest Eocene and that Hyainailourinae originated in Afro-Arabia during the late early Eocene before dispersing to the northern continents. The hyainailourine clade that includes *Simbakubwa* and *Hyainailouros* likely originated in Afro-Arabia during the early Oligocene (C). *Apterodon* appears to have dispersed from Afro-Arabia to Europe during the early Oligocene, and it is possible that *Hyainailouros* could have dispersed during this interval as well. It is more likely that *Hyainailouros sulzeri* dispersed to Europe during the early Miocene (D). Analyses indicate that during the early Miocene, the *H. bugtiensis* clade, *Metapterodon*, and the teratodontine *Dissopsalis* dispersed to southwestern Asia. These dispersal events suggest that Afro-Arabia was an important locus of hyaenodont diversification and that Afro-Arabian lineages were capable of integrating into northern ecosystems that included carnivorans. Cenozoic maps are based on Seton et al. (2012) as rendered in GPlates 2.0 (Earthbyte Group, 2016).

shares features with that of *Hyainailouros sulzeri*, a species known from a complete foot described by Ginsburg (1980). Ginsburg (1980) inferred that *Hyainailouros* was a terrestrial carnivore with a semidigitigrade to plantigrade foot posture. Ginsburg (1980) further hypothesized that *Hyainailouros* was capable of powerful leaps based on its long tuber calcanei. The tuber calcanei of *Simbakubwa* is somewhat shorter, although not as gracile as that of *Kerberos* (Solé et al., 2015), a taxon reconstructed as more plantigrade in posture. Based on calcaneal morphology, *Simbakubwa* likely maintained a semidigitigrade posture.

The hyainailourine shift from a plantigrade posture in *Kerberos* to a semidigitigrade posture in *Simbakubwa* and/or

Hyainailouros should be more closely examined to test whether this locomotor change correlates with environmental change around the Paleogene-Neogene boundary. Digitigrade carnivores are generally found in more open environments (Polly, 2010) where the more efficient, upright foot posture allows carnivores to conserve energy, a particularly important adaptation for large carnivores that range over significant distances (Carbone et al., 2005, 2007). Neither *Simbakubwa* nor *Hyainailouros* is fully digitigrade, but their semidigitigrade posture would have been more efficient than the plantigrade posture of *Kerberos*.

The last hyaenodonts, including *Hyainailouros* in Eurasia, *Megistotherium* in Afro-Arabia, and *Hyaenodon gigas* and *Hyaenodon*

weilini in Asia (Wang et al., 2005), were among the largest hyaenodonts that ever existed (Morlo et al., 2010). Smaller hyaenodonts such as *Dissopsalis* and *Metapterodon* cf. (Barry, 1980, 1988) also persisted into the Miocene, but massive hyaenodonts were found across multiple continents. Several authors (e.g., Van Valkenburgh, 1990; Morlo et al., 2010) have explained this pattern by showing that open environments support taxa with larger body masses (Coe, 1980; Western, 1980). In this scenario, Miocene habitats supported larger herbivores, which were in turn preyed upon by larger carnivores than might be supported in more densely forested ecosystems. Essentially, hyainailourines may have simply become larger as their prey became larger, an idea that can be rigorously tested with the development of better-resolved phylogenies of African herbivores through this interval. Savage (1973) supported the relationship between hyainailourine size and prey size by calculating the gape of *Megistotherium* that could engulf a proboscidean's limb. The relationship between carnivore body mass and prey body mass has been explored in Carnivora, and, indeed, Carbone et al. (1999, 2007) found that carnivores larger than 25 kg generally hunt prey greater than or equal to their own body mass. *Simbakubwa* was close to the size of large anthracotheres (Holroyd et al., 2010) and small proboscideans (Sanders et al., 2010) and may have been the only meat eater on the landscape capable of preying upon such large herbivores.

If *Simbakubwa* and its relatives hunted and scavenged proboscideans and rhinoceroses—prey typically ignored by carnivorans—by exploiting large body size, then hyainailourines may have survived into the Neogene by occupying a specialized predatory niche that remains largely unoccupied in modern ecosystems populated by more socially complex, but smaller carnivorans. Large herbivores tend to have slow generation times (Cardillo et al., 2005), and their populations may be particularly sensitive to environmental change. If large herbivore populations declined, even briefly, during the turbid late Miocene, the large specialized hyaenodonts may have been particularly affected by changing resources, more so than smaller carnivorans. A similar pattern can be observed in modern ecosystems because large hypercarnivores are more dramatically affected by environmental changes than small mesocarnivores (Carbone et al., 2007; Roemer et al., 2009). Cooperative carnivorans with larger, more complex brains also may have become increasingly adept at stealing large carcasses from solitary hyaenodonts, providing a tipping point for large hyainailourines in obtaining adequate amounts of food for survival (Macdonald, 1983; Van Valkenburgh, 2001).

The diets of hyainailourines are often reconstructed to include significant bone processing due to heavy premolar wear and the presence of zigzag Hunter-Schreger bands on the teeth of many taxa (Solé et al., 2015). Compared with the upper molars of *Hyainailouros napakensis*, *H. bugtiensis*, and *H. sulzeri*, the upper molar metastyles of *Simbakubwa* are relatively elongate and gracile, p4 is buccolingually compressed, and the p4 talonid is sectorial. The relatively gracile dentition of *Simbakubwa* seems less adapted for processing bone than the dentition of later Miocene hyainailourines. In relatively mature specimens of *Hyainailouros sulzeri* and *H. bugtiensis*, the buccolingually stout metastyle on M1 and M2 is heavily worn on its lingual face. The robust metastyles that help distinguish *Simbakubwa* from *Hyainailouros* may reflect an adaptation to the heavy wear that accompanies powerful oral processing, with the wider metastyle of *Hyainailouros* providing more enamel to abrade, thus extending the usefulness of the carnassial blade as it is honed throughout an individual's lifetime. The stout metastyles of *Hyainailouros* are convergent with the lingually rotating carnassial blades found in some species of *Hyaenodon* (Mellett, 1977), with both molar adaptations ensuring the metastyle retains a shearing blade that is constantly honed. This change in dental morphology from *Simbakubwa* to *Hyainailouros*, and its correlation with a more expansive diet in the later Miocene, demonstrates that hyainailourines continued to adapt to changing

environmental challenges through the early Neogene as both efficient hunters and scavengers.

As the fossil record of Hyainailourinae improves with the discovery of new taxa such as *Simbakubwa*, so too does our understanding of the dynamic early Neogene world. Massive hyainailourines such as *Megistotherium* and *Hyainailouros* were not part of a fading, defeated endemic Afro-Arabian fauna, but rather hyainailourines and the rest of the Afro-Arabian fauna were integral components in a network of ecosystems in flux as Afro-Arabian flora and fauna met and integrated with Eurasian taxa. Out of the Miocene—the epoch that saw the diversification of our hominoid relatives—the modern Old World ecosystem emerged, fundamentally shaped by gigantic carnivores such as *Simbakubwa* and its hyainailourine kin.

ACKNOWLEDGMENTS

We dedicate this paper to the memory of our mentor and colleague G. Gunnell. We thank M. Munguu, R. Nyaboke, J. Kibii, and F. K. Manthi for access to collections at the KNM. E. Seiffert (USC), J. Barry (Harvard), and T. Lehman (NMSF) provided important discussion and support. We thank C. Argot and G. Billet (MNHN), M. Brett-Surman (NMNH), P. Brewer (NHMUK), J. Chupasko (MCZ), L. Costeur (Naturhistorisches Museum, Basel), J. Cundi (MCZ), J. Galkin (AMNH), G. Gunnell (DPC), M. Hellmund (Geiseltal Museum, Halle), J. Hooker (NHMUK), A. Lavrov (PIN), C. Norris (YPM), S. Pierce (MCZ), C. Riddle (DPC), B. Sanders (University of Michigan), S. Schaal (NMSF), A. Sileem (CGM), T. Smith (IRSNB), F. Solé (IRSNB), G. Rössner (BSPG), A. Vogel (NMSF), E. Westwig (AMNH), N. Xijun (IVPP), and R. Ziegler (SMNS) for access to specimens used in comparative studies. L. Werdelin, J. Meachen, and anonymous reviewers provided useful comments. This paper is a contribution to the REACHE collaborative network, and to the project BR/121/A3/PALEURAFRICA of the Belgian Science Policy Office. NSF grant BCS-1127164, BCS-1638796, and EAR-1349825 to N.J.S. and DBI-1612062 to M.R.B. supported this research.

ORCID

Matthew R. Borths  <https://orcid.org/0000-0002-3840-5308>
Nancy J. Stevens  <http://orcid.org/0000-0002-2402-6526>

LITERATURE CITED

- Anders, U., W. von Koenigswald, I. Ruf, and B. H. Smith. 2011. Generalized individual dental age stages for fossil and extant placental mammals. *Paläontologische Zeitschrift* 85:321–339.
- Andrews, C. W. 1904. Further notes on the mammals of the Eocene of Egypt. *Geological Magazine* 5:109–115, 157–162.
- Andrews, C. W. 1906. A Descriptive Catalogue of the Tertiary Vertebrata of the Fayum, Egypt. British Museum of Natural History, London, 324 pp.
- Andrews, P., T. Harrison, L. Martin, and M. Pickford. 1981. Hominoid primates from a new Miocene locality named Meswa Bridge in Kenya. *Journal of Human Evolution* 10:123–128.
- Antoine, P.-O., J.-L. Welcomme, L. Marivaux, I. Baloch, M. Benammi, and P. Tassy. 2003. First record of Paleogene Elephantoidea (Mammalia, Proboscidea) from the Bugti Hills of Pakistan. *Journal of Vertebrate Paleontology* 23:977–980.
- Argot, C. 2010. Morphofunctional analysis of the postcranium of *Amphicyon major* (Mammalia, Carnivora, Amphicyonidae) from the Miocene of Sansan (Gers, France) compared to three extant carnivores: *Ursus arctos*, *Panthera leo*, and *Canis lupus*. *Geodiversitas* 32:65–106.
- Barry, J. C. 1980. Occurrence of a hyaenodontine creodont (Mammalia) in the late Miocene of Pakistan. *Journal of Paleontology* 54:1128–1131.

- Barry, J. C. 1988. *Dissopsalis*, a middle and late Miocene proviverrine creodont (Mammalia) from Pakistan and Kenya. *Journal of Vertebrate Paleontology* 8:25–45.
- Beck, R. M. D., and M. S. Y. Lee. 2014. Ancient dates or accelerated rates? Morphological clocks and the antiquity of placental mammals. *Proceedings of the Royal Society B: Biological Sciences* 281:20141278.
- Biedermann, W. G. A. 1863. Petrefacten aus der Umgegend von Winterthur. II Heft: Die Braunkohlen von Elgg. Anhang: *Hyainailouros sulzeri*. Bleuler-Hausheer, Winterthur, 23 pp.
- Borths, M. R., and E. R. Seiffert. 2017. Craniodental and humeral morphology of a new species of *Masrasetor* (Teratodontinae, Hyaenodonta, Placentalia) from the late Eocene of Egypt and locomotor diversity in hyaenodonts. *PLoS ONE* 12:e0173527.
- Borths, M. R., and N. J. Stevens. 2017a. The first hyaenodont form the late Oligocene Nsungwe Formation of Tanzania: insights into the Paleogene-Neogene carnivore transition. *PLoS ONE* 12:e0185301. doi:10.1371/journal.pone.0185301.
- Borths, M. R., and N. J. Stevens. 2017b. Taxonomic affinities of the enigmatic *Prionogale breviceps*, early Miocene, Kenya. *Historical Biology*. doi:10.1080/08912963.2017.1393075.
- Borths, M. R., P. A. Holroyd, and E. R. Seiffert. 2016. Hyainailourinae and Teratodontinae cranial material from the late Eocene of Egypt and the application of parsimony and Bayesian methods to the phylogeny and biogeography of Hyaenodonta (Placentalia, Mammalia). *PeerJ* 4:e2639. doi:10.7717/peerj.2639.
- Carbone, C., A. Teacher, and J. M. Rowcliffe. 2007. The costs of carnivory. *PLoS Biology* 5:e22. doi:10.1371/journal.pbio.0050022.
- Carbone, C., G. Cowlishaw, N. J. B. Isaac, and J. M. Rowcliffe. 2005. How far do animals go? Determinants of day range in mammals. *American Naturalist* 165:290–297.
- Carbone, C., G. M. Mace, S. C. Roberts, and D. W. Macdonald. 1999. Energetic constraints on the diet of terrestrial carnivores. *Nature* 402:286–288.
- Cardillo, M., G. M. Mace, K. E. Jones, J. Bielby, O. R. P. Bininda-Emonds, W. Sechrest, C. D. L. Orme, and A. Purvis. 2005. Multiple causes of high extinction risk in large mammal species. *Science* 309:1239–1241.
- Coe, M. 1980. The role of modern ecological studies in the reconstruction of paleoenvironments in sub-Saharan Africa; pp. 55–71 in A. K. Behrensmeyer and A. P. Hill (eds.), *Fossils in the Making*. University of Chicago Press, Chicago, Illinois.
- Delignette-Muller, M. L., and C. Dutang. 2015. fitdistrplus: an R package for fitting distributions. *Journal of Statistical Software* 64(4):1–34.
- Dembo, M., N. J. Matzke, A. Ø. Mooers, and M. Collard. 2015. Bayesian analysis of a morphological supermatrix sheds light on controversial fossil hominin relationships. *Proceedings of the Royal Society B: Biological Sciences* 282:20150943. doi:10.1098/rspb.2015.0943.
- Earthbyte Group. 2016. GPlates 2.0. Available at www.earthbyte.org/gplates-2-0-software-and-data-sets. Accessed April 14, 2018.
- Egi, N. 2001. Body mass estimates in extinct mammals from limb bone dimensions: the case of North American hyaenodontids. *Paleontology* 44:497–528.
- Egi, N., T. Tsubamoto, and M. Takai. 2007. Systematic status of Asian “*Pterodon*” and early evolution of hyaenaelurine hyaenodontid creodonts. *Journal of Paleontology* 81:770–778.
- Evans, E. M. N., J. A. H. Van Couvering, and P. Andrews. 1981. Palaeoecology of Miocene sites in Western Kenya. *Journal of Human Evolution* 10:99–116.
- Frischia, A., and B. Van Valkenburgh. 2010. Ecomorphology of North American Eocene carnivores: evidence for competition between carnivorans and creodonts; pp. 311–241 in A. Goswami and A. Frischia (eds.), *Carnivoran Evolution: New Views on Phylogeny, Form, and Function*. University Press Cambridge, Cambridge, U.K.
- Gheerbrant, E., and J.-C. Rage. 2006. Paleobiogeography of Africa: how distinct from Gondwana and Laurasia. *Palaeogeography, Palaeoclimatology, Palaeoecology* 241:224–246.
- Ginsburg, L. 1980. *Hyainailouros sulzeri*, mammifère créodonte du Miocène d’Europe. *Annales de Paléontologie* 66:19–73.
- Gittleman, J. L. 1995. Carnivore body size: ecological and taxonomic correlates. *Oecologia* 67:540–554.
- Gorscak, E., and P. M. O’Connor. 2016. Time-calibrated models support congruency between Cretaceous continental rifting and titanosaurian evolutionary history. *Biology Letters* 12:20151047. doi:10.1098/rsbl.2015.1047.
- Gunderson, A. 2009. *Ursus maritimus*. Animal Diversity Web. Available at animaldiversity.org/accounts/Ursus_maritimus. Accessed March 7, 2018.
- Gunnell, G. F. 1998. Creodonta; pp. 91–109 in C. M. Janis, K. M. Scott, and L. L. Jacobs (eds.), *Evolution of Tertiary Mammals of North America. Volume 1: Terrestrial Carnivores, Ungulates, and Ungulate-like Mammals*. Cambridge University Press, Cambridge, U.K.
- Harrison, T., and P. Andrews. 2009. The anatomy and systematic position of the early Miocene proconsulid from Meswa Bridge, Kenya. *Journal of Human Evolution* 56:479–496.
- Heritage, S., D. Fernández, H. M. Sallam, D. T. Cronin, J. M. E. Echube, and E. R. Seiffert. 2016. Ancient phylogenetic divergence of the enigmatic African rodent *Zenkerella* and the origin of anomaluroid gliding. *PeerJ* 4:e2320. doi:10.7717/peerj.2320.
- Holliday, J. A., and S. J. Steppan. 2004. Evolution of hypercarnivory: the effect of specialization on morphological and taxonomic diversity. *Paleobiology* 30:108–128.
- Holroyd, P. A. 1999. New Pterodontinae (Creodonta: Hyaenodontidae) from the late Eocene–early Oligocene Jebel Qatrani Formation, Fayum Province, Egypt. *PaleoBios* 19(2):1–18.
- Holroyd, P. A., F. Lihoreau, G. F. Gunnell, and E. Miller. 2010. Anthracotheriidae; pp. 851–859 in L. Werdelin and W. Sanders (eds.), *Cenozoic Mammals of Africa*. University of California Press, Berkeley, California.
- Hooijer, D. A. 1963. Miocene Mammalia of Congo. *Annales, Musée royal de l’Afrique Centrale, Ser. in 8°* 46:1–77.
- Huxley, T. H. 1880. On the application of the laws of evolution to the arrangement of the Vertebrata, and more particularly of the Mammalia. *Proceedings of the Zoological Society, London* 43:649–662.
- Lange-Badré, B. 1979. Les créodontes (Mammalia) d’Europe occidentale de l’Éocène supérieur à l’Oligocène supérieur. *Mémoires du Muséum national d’Histoire naturelle* 42:1–249.
- Lewis, M. E., and M. Morlo. 2010. Creodonta; pp. 543–560 in L. Werdelin and W. Sanders (eds.), *Cenozoic Mammals of Africa*. University of California Press, Berkeley, California.
- Linnaeus, C. 1758. *Systema Naturae per Regna Tria Naturae, Secundum Classes, Ordines, Genera, Species, cum Characteribus, Differentiis, Synonymis, Locis*. Tomus I. Editio decima, reformata. Laurentii Salvii, Stockholm, 824 pp.
- Lund, E. K., P. M. O’Connor, M. A. Loewen, and Z. A. Jinnah. 2016. A new centrosaurine ceratopsid, *Machairoceratops cronusi* gen et sp. nov., from the Upper Sand Member of the Wahweap Formation (Middle Campanian), southern Utah. *PLoS ONE* 11:e0154403. doi:10.1371/journal.pone.0154403.
- MacDonald, D. W. 1983. The ecology of carnivore social behaviour. *Nature* 301:379–384.
- Maddison, W. P., and D. R. Maddison. 2016. Mesquite: a modular system for evolutionary analysis. Version 3.10. Available at mesquiteproject.org. Accessed March 11, 2018.
- Matthew, W. D. 1909. The Carnivora and Insectivora of the Bridger Basin, middle Eocene. *Memoirs of the American Museum of Natural History* 9:289–567.
- Mellet, J. S. 1969. A skull of *Hemipsalodon* (Mammalia, Deltatheridia) from the Clarno Formation of Oregon. *American Museum Novitates* 387:1–19.
- Mellet, J. S. 1977. Paleobiology of North American Hyaenodon (Mammalia, Creodonta). *Contributions to Vertebrate Evolution* 1:1–134.
- Morales, J., and M. Pickford. 2017. New hyaenodonts (Ferae, Mammalia) from the early Miocene of Napak (Uganda), Koru (Kenya) and Grullental (Namibia). *Fossil Imprint* 73:332–359.
- Morales, J., M. Pickford, and D. Soria. 2007. New carnivoran material (Creodonta, Carnivora and incertae sedis) from the early Miocene of Napak, Uganda. *Paleontological Research* 11:71–84.
- Morales, J., M. Pickford, D. Soria, and S. Fraile. 1998. New carnivores from the basal Middle Miocene of Arrisdrift, Namibia. *Eclogae Geologicae Helveticae* 91:27–40.
- Morales, J., M. Pickford, S. Fraile, M. J. Salesa, and D. Soria. 2003. Creodonta and Carnivora from Arrisdrift, early Middle Miocene of Southern Namibia. *Memoir of the Geological Survey of Namibia* 19:177–194.
- Morlo, M. 1999. Niche structure and evolution in creodont (Mammalia) faunas of the European and North American Eocene. *Geobios* 32:297–305.

- Morlo, M., G. Gunnell, and D. Nagel. 2010. Ecomorphological analysis of carnivore guilds in the Eocene through Miocene of Laurasia; pp. 269–311 in A. Goswami and A. Friscia (eds.), *Carnivoran Evolution: New Views on Phylogeny, Form, and Function*. Cambridge University Press, Cambridge, U.K.
- Morlo, M., E. R. Miller, and A. N. El-Barkooky. 2007. Creodonta and Carnivora from Wadi Moghra, Egypt. *Journal of Vertebrate Paleontology* 27:145–159.
- Paradis, E., J. Claude, and K. Strimmer. 2004. APE: analyses of phylogenetics and evolution in R language. *Bioinformatics* 20:289–290.
- Partridge, T. C. 2010. Tectonics and geomorphology of Africa during the Phanerozoic; pp. 3–17 in L. Werdelin and W. Sanders (eds.), *Cenozoic Mammals of Africa*. University of California Press, Berkeley, California.
- Pickford, M. 1984. Kenya Palaeontology Gazetteer: Western Kenya. National Museums of Kenya, Special Publication 1:1–282.
- Pickford, M., and P. Tassy. 1980. A new species of *Zygodontophodon* (Mammalia, Proboscidea) from the Miocene hominoid localities of Meswa Bridge and Moroto (East Africa). *Neues Jahrbuch für Geologie und Paläontologie, Monatshefte* 4:235–251.
- Pilgrim, G. E. 1912. The Vertebrate Fauna of the Gaj Series in the Bugti Hills and the Punjab. Memoir of the Geological Survey of India, *Palaeontologia Indica*, New Series 4:1–83.
- Pilgrim, G. E. 1932. The fossil Carnivora of India. *Memoirs of the Geological Survey of India, Palaeontologia Indica*, New Series 18:1–232.
- Pires, M. M., D. Silvestro, and T. B. Quental. 2017. Interactions within and between clades shaped the diversification of terrestrial carnivores. *Evolution* 71:1855–1864.
- Polly, P. D. 1996. The skeleton of *Gazinyocyon vulpeculus* gen. et comb. nov. and the cladistic relationships of Hyaenodontidae (Eutheria, Mammalia). *Journal of Vertebrate Paleontology* 16:303–319.
- Polly, P. D. 2010. Tiptoeing through the trophics: geographic variation in carnivorous locomotor ecomorphology in relation to environment; pp. 374–410 in A. Goswami and A. Friscia (eds.), *Carnivoran Evolution: New Views on Phylogeny, Form, and Function*. Cambridge University Press, Cambridge, U.K.
- Rambaut, A. 2016. FigTree v1.4.3. Available at tree.bio.ed.ac.uk/software/figtree/. Accessed March 7, 2018.
- Rana, R. S., K. Kumar, S. P. Zack, F. Solé, K. D. Rose, P. Missiaen, L. Singh, A. Sahni, and T. Smith. 2015. Craniodental and postcranial morphology of *Indohyaenodon raoi* from the early Eocene of India, and its implications for ecology, phylogeny, and biogeography of hyaenodontid mammals. *Journal of Vertebrate Paleontology*. doi:10.1080/02724634.2015.965308.
- Rasmussen, D. T., and M. Gutiérrez. 2009. A mammalian fauna from the late Oligocene of northwestern Kenya. *Palaeontographica, Abteilung A* 288:1–52.
- Rasmussen, D. T., C. D. Tilden, and E. L. Simons. 1989. New specimens of the giant creodont *Megistotherium* (Hyaenodontidae) from Moghara, Egypt. *Journal of Mammalogy* 70:442–447.
- Roberts, E. M., N. J. Stevens, P. M. O'Connor, P. Dirks, M. D. Gottfried, W. C. Clyde, R. A. Armstrong, A. I. S. Kemp, and S. Hemming. 2012. Initiation of the western branch of the East African Rift coeval with the eastern branch. *Nature Geoscience* 5:289–294.
- Roemer, G. W., M. E. Gompper, and B. Van Valkenburgh. 2009. The ecological role of the mesocarnivore. *BioScience* 59:165–173.
- Ronquist, F., M. Teslenko, P. van der Mark, D. L. Ayres, A. Darling, S. Höhna, B. Larget, L. Liu, M. A. Suchard, J. P. Huelsenbeck. 2012. MrBayes 3.2: efficient Bayesian phylogenetic inference and model choice across a large model space. *Systematic Biology* 61:539–542.
- Rose, K. 2006. *The Beginning of the Age of Mammals*. Johns Hopkins University Press, Baltimore, Maryland, 448 pp.
- Rössner, G. E., and K. Heissig (eds.). 1999. *The Miocene Land Mammals of Europe*. Verlag Dr. Friedrich Pfeil, Munich, Germany, 516 pp.
- Sallam, H. M., and E. R. Seiffert. 2016. New phiomorph rodents from the latest Eocene of Egypt, and the impact of Bayesian “clock”-based phylogenetic methods on estimates of basal hystricognath relationships and biochronology. *PeerJ* 4:e1717. doi:10.7717/peerj.1717.
- Sanders, W. J., E. Gheerbrant, J. M. Harris, H. Saegusa, and C. Delmer. 2010. Proboscidea; pp. 161–251 in L. Werdelin and W. Sanders (eds.), *Cenozoic Mammals of Africa*. University of California Press, Berkeley, California.
- Savage, R. J. G. 1965. Fossil mammals of Africa 19: the Miocene Carnivora of East Africa. *Bulletin of the British Museum of Natural History (Geology)* 10(8):239–316.
- Savage, R. J. G. 1973. *Megistotherium*, gigantic hyaenodont from Miocene of Gebel Zelten, Libya. *Bulletin of the British Museum of Natural History (Geology)* 22:483–511.
- Schaller, G. 1972. *The Serengeti Lion*. The University of Chicago Press, Chicago, Illinois, 504 pp.
- Schlosser, M. 1911. Beiträge zur Kenntnis der oligozänen Landsäugetiere aus dem Fayum, Ägypten. *Beiträge zur Paläontologie und Geologie Österreich-Ungarns, Wien* 14:51–167.
- Schneider, C. A., W. S. Rasband, K. W. Eliceiri. 2012. NIH Image to ImageJ: 25 years of image analysis. *Nature Methods* 9:671–675.
- Sen, S. 2013. Dispersal of African mammals in Eurasia during the Cenozoic: ways and whys. *Geobios* 46:159–172.
- Sepulchre, P., G. Ramstein, F. Fluteau, M. Schuster, J.-J. Tiercelin, and M. Brunet. 2006. Tectonic uplift and eastern Africa aridification. *Science* 313:1419–1423.
- Seton, M., R. D. Müller, S. Zahirovic, C. Gaina, T. H. Torsvik, G. Shephard, A. Talsma, M. Gurnis, M. Turner, S. Maus, and M. Chandler. 2012. Global continental and ocean basin reconstructions since 200 Ma. *Earth-Science Reviews* 113:212–270.
- Solé, F., E. Amson, M. R. Borths, D. Vidalenc, M. Morlo, and K. Bastl. 2015. A new large hyainailourine from the Bartonian of Europe and its bearings on the evolution and ecology of massive hyaenodonts (Mammalia). *PLoS ONE* 10:e141941. doi:10.1371/journal.pone.0135698.
- Solé, F., J. Lhuillier, M. Adaci, M. Bensalah, M. Mahboubi, and R. Tabuce. 2014. The hyaenodontidans from the Gour Lazib area (?early Eocene, Algeria): implications concerning the systematics and the origin of the Hyainailourinae and Teratodontinae. *Journal of Systematic Palaeontology* 12:303–322.
- Sorkin, B. 2008. A biomechanical constraint on body mass in terrestrial mammalian predators. *Lethaia* 41:333–347.
- Stevens, N. J., E. R. Seiffert, P. M. O'Connor, E. M. Roberts, M. D. Schmitz, C. Krause, E. Gorscak, S. Ngasala, T. L. Hieronymus, and J. Temu. 2013. Palaeontological evidence for an Oligocene divergence between Old World monkeys and apes. *Nature* 497:611–614.
- Tassy, P., and M. Pickford. 1983. Un nouveau mastodonte zygodontophonte (Proboscidea, Mammalia) dans le Miocène inférieur d'Afrique orientale: systématique et paléoenvironnement. *Geobios* 16:53–77.
- Van der Made, J. 1999. Intercontinental relationship Europe-Africa and the Indian subcontinent; pp. 457–472 in G. Rössner and K. Heissig (eds.), *The Miocene Land Mammals of Europe*. Verlag Dr. F. Pfeil, Munich, Germany.
- Van Valen, L. 1967. New Paleocene insectivores and insectivore classification. *Bulletin of the American Museum of Natural History* 135:217–284.
- Van Valkenburgh, B. 1990. Skeletal and dental predictors of body mass in carnivores; pp. 181–206 in J. Damuth and B. J. MacFadden (eds.), *Body Size in Mammalian Paleobiology: Estimation and Biological Implications*. Cambridge University Press, New York.
- Van Valkenburgh, B. 2001. The dog-eat-dog world of carnivores: a review of past and present carnivore community dynamics; pp. 101–121 in C. B. Stanford and H. T. Bunn (eds.), *Meat-Eating and Human Evolution*. Oxford University Press, New York.
- Van Valkenburgh, B. 2007. Déjà vu: the evolution of feeding morphologies in the Carnivora. *Integrative and Comparative Biology* 47:147–163.
- Wang, X., Z. Qiu, and B. Wang. 2005. Hyaenodonts and carnivorans from the early Oligocene to early Miocene of Xianshuihe Formation, Lanzhou Basin, Gansu Province, China. *Palaeontologia Electronica* 8(1):6A.
- Werdelin, L. 2010. Chronology of Neogene mammal localities; pp. 27–43 in L. Werdelin and W. J. Sanders (eds.), *Cenozoic Mammals of Africa*. University of California Press, Berkeley, California.
- Werdelin, L., and S. Peigné. 2010. Carnivora; pp. 609–663 in L. Werdelin and W. J. Sanders (eds.), *Cenozoic Mammals of Africa*. University of California Press, Berkeley, California.
- Western, D. 1980. Linking the ecology of past and present mammal communities; pp. 41–54 in A. K. Behrensmeyer and A. P. Hill (eds.), *Fossils in the Making*. University of Chicago Press, Chicago, Illinois.

- Yoder, A. D., M. M. Burns, S. Zehr, T. Delefosse, G. Veron, S. M. Goodman, and J. J. Flynn. 2003. Single origin of Malagasy Carnivora from an African ancestor. *Nature* 421:734–737.
- Yu, Y., A. J. Harris, C. Blair, and X. He. 2015. RASP (Reconstruct Ancestral State in Phylogenies): a tool for historical biogeography. *Molecular Phylogenetics and Evolution* 87:46–49.
- Zachos, J., M. Pagani, L. Sloan, E. Thomas, and K. Billups. 2001. Trends, rhythms, and aberrations in global climate 65 Ma to present. *Science* 292:686–693.
- Submitted May 22, 2018; revisions received December 13, 2018; accepted December 18, 2018.
Handling editor: Julie Meachen.